



A Literature Review of Radiation Damage Data for Copper and Copper Alloys

S.J. Zinkle and R.W. Knoll

May 1984

UWFDM-578

FUSION TECHNOLOGY INSTITUTE
UNIVERSITY OF WISCONSIN
MADISON WISCONSIN

DISCLAIMER

This report was prepared as an account of work sponsored by an agency of the United States Government. Neither the United States Government, nor any agency thereof, nor any of their employees, makes any warranty, express or implied, or assumes any legal liability or responsibility for the accuracy, completeness, or usefulness of any information, apparatus, product, or process disclosed, or represents that its use would not infringe privately owned rights. Reference herein to any specific commercial product, process, or service by trade name, trademark, manufacturer, or otherwise, does not necessarily constitute or imply its endorsement, recommendation, or favoring by the United States Government or any agency thereof. The views and opinions of authors expressed herein do not necessarily state or reflect those of the United States Government or any agency thereof.

A Literature Review of Radiation Damage Data for Copper and Copper Alloys

S.J. Zinkle and R.W. Knoll

Fusion Technology Institute
University of Wisconsin
1500 Engineering Drive
Madison, WI 53706

<http://fti.neep.wisc.edu>

May 1984

UWFDM-578

A LITERATURE REVIEW OF RADIATION DAMAGE DATA
FOR COPPER AND COPPER ALLOYS

S.J. Zinkle and R.W. Knoll[†]

Fusion Engineering Program
Nuclear Engineering Department
University of Wisconsin-Madison
Madison, Wisconsin 53706

June 1984

UWFD-578

[†]Present Address: Battelle Northwest Laboratory, Richland, WA 99352.

TABLE OF CONTENTS

	<u>PAGE</u>
I. Introduction.....	1
II. Solute Segregation and Phase Stability Experiments.....	3
III. Void and Loop Studies.....	27
A. Neutron Irradiations.....	27
B. Electron Irradiations.....	38
C. Ion Irradiations.....	54
IV. Fundamental Studies: Radiation Hardening and Resistivity Changes..	73
V. Concluding Remarks.....	81
References.....	83

I. Introduction

Copper and its alloys have been the subject of many radiation damage studies over the years, and they have recently received renewed attention due to fusion design studies which call for incorporation of copper and copper alloys into future fusion reactors.⁽¹⁾ Many of the early fundamental studies on radiation damage in metals were conducted on copper. This was due to the fact that copper is an fcc metal with a well-established metallurgy, it is conducive to fabrication and examination, and it has a large data base of its unirradiated properties. Much of the early work on irradiated copper used resistivity and hardness measurements as a means to detect lattice damage, and was summarized by Corbett⁽²⁾ in 1966. Recent experiments have been performed on irradiated copper using such tools as transmission electron microscopy (TEM), tensile tests, microhardness tests, x-ray diffuse scattering, positron annihilation, Mössbauer spectroscopy and Auger electron spectroscopy.

Knoll⁽³⁾ surveyed the copper radiation damage literature in 1980 and summarized the void and loop formation results obtained up to that time. A large number of new investigations on the irradiated behavior of copper and copper alloys have recently appeared in the literature. The present review contains an extensive section on experiments examining solute segregation and phase stability of copper alloys during irradiation. This information was not contained in Knoll's review, largely because most of these studies have only recently been published. The present review has incorporated all of the information contained in Knoll's review,⁽³⁾ and is therefore intended to supercede this older report.

The list of references contained herein should not be taken as being all-inclusive. For example, this review does not address any of the numerous

sputtering or blistering experiments which have been reported for copper and/or copper alloys. There are many additional reported copper irradiation experiments which have not been cited simply because they are either summaries of results which have been obtained by several other investigators, or results which were later extended.

Recent work by several research groups has shown the displacement efficiency (K) factor used to calculate dpa values exhibits a variation with respect to recoil energy (see Kinney et al.⁽⁴⁾ for a recent review.) This is in contrast to the "standard" value of $K = 0.8$ used in the modified Kinchin-Pease model.⁽⁵⁾ In order to better facilitate correlations between various irradiating species, this review has modified the reported dpa values to bring them into agreement with the current understanding of displacement damage: $K \approx 0.8$ for electron irradiations, $K \approx 0.3$ for fast neutron and high energy (≥ 500 keV) heavy ion irradiations, and $K =$ intermediate values for light ion and low energy heavy ion irradiations.

It is difficult to establish an exact damage level per unit fluence for neutron irradiations due to the fact that the dpa level depends upon the neutron energy spectrum. Only a rough comparison of the dpa level from one study to another can be made unless the respective neutron spectra have been fully characterized. For convenience, we have made estimates of the neutron damage levels from reported fluences in the cases where dpa values were not given. A fission neutron fluence of 1×10^{26} n/m² ($E > 1$ MeV) corresponds to roughly 4 dpa ($K = 0.3$), and a moderated fission neutron fluence of 1×10^{26} n/m² ($E > 0.1$ MeV) \approx 3 dpa ($K = 0.3$). The above correlations were made assuming a displacement energy for copper of 29 eV and spectral averaged damage energies of 81 keV-b and 56 keV-b for neutron fluences of $E > 1$ MeV and of $E > 0.1$ MeV, respectively.⁽⁶⁾

The first section of this review deals with solute segregation and radiation-induced precipitation experiments conducted in copper alloys. The second section reviews void and loop formation studies. Data from neutron, ion and electron irradiations are surveyed separately. The final section briefly reviews some recent fundamental irradiation studies on copper and copper alloys which do not fall under either of the two headings above.

II. Solute Segregation and Phase Stability Experiments

Numerous studies of segregation and precipitation in irradiated Cu alloys have been performed. Corbett⁽²⁾ surveyed the results from early resistivity studies on irradiated copper alloys. Adda et al.⁽⁶⁴⁾ tabulated the experimental observations of radiation-enhanced diffusion, precipitation and ordering effects for copper alloys in 1975. Knoll⁽⁷⁾ has reviewed some of the phase stability experiments, concentrating on the data obtained from Cu-Be, Cu-Co and Cu-Fe. Russell⁽⁸⁾ has recently summarized much of the published work on irradiation enhanced/induced precipitation and solute segregation. The observed segregation effects in alloys are related to differences in atomic size between the solvent and solute atoms. King⁽⁹⁾ has published atomic size misfit values for alloys based on precision lattice parameter measurements. The results of solute segregation and phase stability experiments for sixteen irradiated copper alloys are summarized in Table 1.

II.A. Cu-Ag

Takahashi and co-workers^(10,11) irradiated supersaturated Cu-2% Ag in a 650 keV HVEM. Irradiation to 10 dpa at a temperature of 523 K caused radiation-enhanced precipitation near grain boundaries and the surface of the foil. Solute enrichment peaks on either side of grain boundaries were observed by EDS techniques, with a local depletion right at the grain boundary.

This was interpreted as evidence of solute segregation away from the boundary, which was expected for oversized Ag atoms (size effect/vacancy inverse Kirkendall effect). The Ag concentration was depleted immediately adjacent and far away from voids which were present in the alloy. At intermediate depths, an enhanced Ag solute concentration was observed.

II.B. Cu-Al

Wechsler and Kernohan⁽¹²⁾ were among the first to report on the results of irradiation of copper-base Cu-Al alloys. They studied the effect of fast neutron irradiation at temperatures of 35°C and -120°C on the electrical resistivity of α -phase Cu-Al alloys. At the higher temperature, the alloy resistivity initially decreased, reached a minimum, and then increased linearly with dose. At the lower temperature, no decrease in resistivity with dose was found. However, the decrease appeared upon subsequent warming above -50°C. Isothermal annealing above 150°C caused the resistivity to increase again. They discussed several mechanisms in an attempt to explain the observed effects, including short-range ordering, clustering, and solute atom-vacancy pairing but no definitive conclusions were reached.

Other investigations^(13,14) determined that irradiation enhanced the thermal aging rate (irradiation-enhanced diffusion) and caused short range ordering. A recent study of Cu-5% Al irradiated with 14-MeV neutrons at room temperature by Zinkle and Kulcinski⁽¹⁵⁾ found that the electrical resistivity initially decreased, reached a minimum, and then increased with dose, in agreement with the Wechsler and Kernohan results. This behavior was attributed to short-range ordering. Thermal annealing studies⁽¹⁶⁾ show evidence of short-range ordering in Cu-Al when annealed below 670 K. Friedman et al.⁽¹⁷⁾ studied the low-temperature thermal conductivity behavior in Cu-Al following

neutron irradiation and suggested that solute segregated around dislocations (point defect sinks).

II.C. Cu-Au (Cu_3Au)

Several investigations have been conducted on Cu-Au alloys, mainly dealing with order-disorder transformations.⁽¹⁸⁻²⁵⁾ Fenzl et al.⁽²⁶⁾ have observed deviations from Matthiessen's rule during neutron irradiation of Cu-Au alloys. Oleownik and Schüle⁽¹⁸⁾ used resistivity techniques to measure radiation-enhanced diffusion in copper-gold alloys containing 10-25 atomic percent gold during neutron and electron irradiations. The mechanism for ordering in Cu_3Au during irradiation was found to change from a vacancy-type to an interstitialcy-type with increasing degree of order. Kirk and Blewitt⁽²⁴⁾ performed an extensive study of the effect of neutron irradiation on order-disorder phase transformations in Cu_3Au . Zee and Wilkes⁽¹⁹⁻²¹⁾ and Guinan and co-workers⁽²²⁾ have experimentally and theoretically investigated the effect of irradiation (electron and neutron) on long range order in Cu_3Au . English and Jenkins⁽²³⁾ used TEM to characterize displacement cascade damage (zones of reduced long range order) in Cu_3Au following 14-MeV and fission neutron irradiation. A more complete discussion of the effects of irradiation on the phase stability of Cu_3Au may be found in Refs. 21, 22, and 25.

II.D. Cu-Be

Several extensive studies have been carried out on the Cu-Be alloy system, in which Be acts as an ideal undersized solute.^(7,27-36,38-43) Murray and Taylor⁽²⁷⁾ studied the resistivity and hardness of Cu-Be as a function of fast neutron dose at temperatures between 0°C and 40°C. They observed large increases in the alloy resistivity and hardness, and deduced that radiation-induced precipitation had occurred. Bystrov et al.⁽²⁸⁾ measured the resis-

tivity of quenched Cu-Be as a function of 2.5 MeV electron irradiation dose up to $\sim 10^{-5}$ dpa. Samples were irradiated at 20°C and then annealed. The observed increase in resistivity was attributed to accelerated decomposition of the solid solution due to an irradiation-produced vacancy/interstitial interaction.

Yoshida and co-workers⁽²⁹⁻³²⁾ made a comprehensive investigation of the effects of neutron irradiation on phase transformation in quenched Cu-Be alloys. The normal sequence of events observed during thermal annealing of Cu-Be is supersaturated $\alpha \rightarrow$ Guinier-Preston (G.P.) zones $\rightarrow \gamma'' \rightarrow \gamma' \rightarrow \gamma$ (an incoherent, stable precipitate). Resistivity measurements combined with TEM indirectly indicated that the resistivity increases previously observed by Murray and Taylor were due to enhanced formation of G.P. zones. The intermediate precipitate γ' was observed in two cases.⁽³¹⁻³²⁾ Post-irradiation aging resulted in enhanced formation of the γ' phase from the G.P. zones. The accelerated G.P. zone formation during irradiation was attributed to radiation-enhanced diffusion and preferential displacement of the light Be atoms. Yoshida has recently summarized these observations of radiation-enhanced G.P. zone formation and γ' precipitation.⁽³³⁾ The Kyoto University report also reviews phase stability results during irradiation of several ternary alloys containing Cu, Be and either Mg, Co, Fe or Zn (data from Refs. 31, 32). Mg and Zn atoms were observed to accelerate the precipitation process, while Co and Fe atoms trapped vacancies and retarded G.P. zone formation and γ precipitation.⁽³³⁾

V. Lensa et al.⁽³⁴⁾ and Bartels et al.⁽³⁵⁾ studied solute segregation in dilute Cu-Be alloys through electrical resistivity changes. Irradiation with 3-MeV electrons at temperatures of 280-410 K caused Be to segregate to inter-

nal point defect sinks. It was estimated that one Be atom was removed from solid solution for every 2-4 Frenkel defect pairs created by the irradiation, indicating a strong segregation mechanism. The solute concentration was found to decrease linearly with irradiation fluence. They attributed the observed solute segregation during irradiation to an interstitialcy (mixed dumbbell) mechanism.

Knoll et al.^(7,36) used Auger electron spectroscopy combined with sputtering and cross-sectional TEM observations to monitor the segregation of Be in the near-surface region following 14-MeV Cu ion irradiation. Irradiation of solution-annealed Cu-Be at temperatures of 350-475°C caused strong irradiation-induced segregation of the undersized Be solute, with the amount of segregation increasing with irradiation temperature and dose. Copious precipitation of CuBe platelets was uniformly induced in the matrix throughout the damage region in both supersaturated and undersaturated Cu-3.4 at % Be. The precipitates had the lattice parameter, crystal structure, and precipitate/matrix orientation of the γ -CuBe equilibrium phase, but were situated on habit planes expected for the γ' -CuBe intermediate phase. Post-irradiation annealing studies proved that the precipitation was radiation-induced as opposed to radiation-enhanced. Precipitate-free zones were occasionally observed at grain boundaries. Precipitate growth appeared to be due to Johnson and Lam's⁽³⁷⁾ solute-drag mechanism, where Be solute atoms preferentially segregate to nucleation sites (point defect sinks) via a strong coupling with the interstitials. The enhanced Be segregation to the irradiated surfaces was attributed to radiation-enhanced diffusion and to oxidation of the Be, as opposed to the solute drag mechanism. There was no evidence of Be segregation within the damage zone (except near the surface). It was suggested that the

presence of the precipitate sinks prevented the long-range migration of interstitials.

Recent studies by Wollenberger and co-workers⁽³⁸⁻⁴²⁾ have used either 300-keV Cu ions or 1-MeV electrons in order to investigate Cu-Be segregation effects during irradiation. The Cu ion irradiation produced homogeneous precipitation of the equilibrium γ phase, with no evidence of the intermediate metastable phases.⁽³⁸⁾ Conversely, electron irradiation produced a precipitation sequence which was the same as that found during thermal annealing (metastable phase formation).⁽³⁹⁾ They proposed that precipitation during ion irradiation was due to Be-interstitial complexes segregating to cascade-induced vacancy loops. The migration/dissociation energies of the complex were estimated,⁽⁴⁰⁾ and radiation-enhanced partial diffusion coefficients were measured using SIMS.⁽⁴¹⁻⁴²⁾ Some evidence of radiation-induced precipitate dissolution via athermal cascade mixing was observed, and the dissolution rate was estimated to be approximately equal to the defect production rate.⁽⁴²⁾ Knoll⁽⁷⁾ has also reported indirect evidence of precipitate dissolution in ion-irradiated Cu-Be.

Kinoshita et al.⁽⁴³⁾ irradiated both under- and oversaturated Cu-Be alloys in a 650 keV HVEM. They found that irradiation of supersaturated Cu-Be reproduced the thermal precipitation sequence with accelerated kinetics -- this result was later confirmed by Wahi et al.⁽³⁹⁾ as described above. Irradiation of the undersaturated Cu-Be alloy produced homogeneous precipitation in the matrix, rather than at point defect sinks where the undersized Be solute would tend to segregate. They proposed that segregation during irradiation of the undersaturated alloy was via a interstitial-Be complex (dumb-bell).

II.E. Cu-Co

Precipitation in Cu-Co alloys is usually in the form of homogeneous, coherent particles. Piercy⁽⁴⁴⁾ used neutron irradiation at 50°C to study the behavior of aged Cu-Co precipitates. Magnetic saturation measurements indicated that the precipitate density decreased in the specimens containing particles smaller than ~ 2.5 nm diameter. Precipitate density increased and the particle size decreased in specimens containing larger particles. These changes were attributed to nucleation of new particles during irradiation. However, irradiation of a quenched and unaged alloy did not yield any measurable particle nucleation. Blaise⁽⁴⁵⁾ examined precipitate formation in supersaturated Cu-1% Co during neutron irradiation at temperatures 40-210°C in order to quantify the effects of radiation-enhanced precipitation versus precipitate dissolution. A comparison was made with non-irradiated control samples, with the result that more precipitation was observed in the irradiated specimens. The precipitate size in the irradiated specimens was essentially constant over the entire temperature range, whereas the control precipitate sizes increased by more than a factor of two. The control and irradiated precipitate sizes were similar at a temperature of about 170°C.

Several workers have used TEM to study radiation-induced coherency loss of Co-rich particles in aged, dilute Cu-Co alloys.^(7,46-48) A neutron-irradiation study by Brown et al.⁽⁴⁶⁾ found that particles larger than 30 nm diameter had lost coherency, while smaller ones had not. A model which analyzed the energetics for coherency loss of the precipitates via creation of a dislocation loop around the particle was found to be in rough agreement with the above experimental results. Woolhouse and co-workers^(47,48) used 450 keV electron (HVEM)⁽⁴⁷⁾ and fast neutron⁽⁴⁸⁾ irradiations to study coherency loss

in a Cu-Co alloy. The HVEM irradiation caused particles of 5 nm diameter and larger to become incoherent due to dislocation loop migration. In the neutron irradiation study, it was observed that the critical size for coherency loss decreased with increasing fluence. Coherency loss during electron irradiation was attributed to migration of irradiation-produced interstitials to the interface followed by prismatic dislocation loop nucleation. Coherency loss during neutron irradiation was proposed to be due to climb and glide of a dislocation to the particle-matrix interface. Knoll⁽⁷⁾ concluded from TEM observations that 14-MeV Cu ion irradiation at 400-475°C on aged Cu-Co caused loss of precipitate coherency due to absorption of free interstitials at the particle-matrix interface. All visible precipitates within the damage zone become incoherent following irradiation to doses as low as 0.1 dpa ($K = 0.3$). Loss of coherency was observed well beyond the damage region (by $\sim 1 \mu\text{m}$), and this was attributed to long range migration of free interstitials originating within the damage zone.

II.F. Cu-Cr

Rovinskii et al.⁽⁴⁹⁾ investigated the microstructure of Cu-0.3% Cr following a CO₂ laser irradiation at a power density of 10^{11} W/m^2 . Grain boundary migration and Cr precipitate dissolution was observed to occur. A mosaic structure formed in the matrix similar to that observed after high-temperature deformation.

II.G. Cu-Fe

A metastable, coherent precipitate (fcc Fe, spherical) forms initially upon aging of copper-base Cu-Fe alloys. Upon further aging, this paramagnetic precipitate transforms to the equilibrium ferromagnetic (bcc Fe) phase and is incoherent. Denney used saturation magnetization techniques to study precipi-

tate transformations during a 0.5 MeV electron⁽⁵⁰⁾ and 9 MeV H⁺ irradiation.⁽⁵¹⁾ He reported that irradiation caused a fcc-to-bcc allotropic transformation in some of the precipitates, and concluded that the proton irradiation caused some precipitate dissolution. Boltax^(52,53) measured electrical resistivity and magnetization changes of aged Cu-Fe specimens as a function of neutron irradiation dose. Samples aged at 300°C (high concentration of small precipitates) underwent a significant resistivity increase (~ 35%) following irradiation with the greatest increase found in samples aged for the shortest times. Samples aged near 700°C exhibited a resistivity decrease following irradiation. Irradiation increased the saturation magnetization, with the greatest increase corresponding to the shorter irradiation times. The resistivity increases were proposed to be due to precipitate dissolution (increased solute in the matrix) and the resistivity decreases were attributed to RIP. The increase in saturation magnetization was suggested to be caused by coherent, paramagnetic precipitates being transformed into incoherent, ferromagnetic precipitates.

Gould and Vincent⁽⁵⁴⁾ used Mössbauer spectroscopy techniques to investigate the relative importance of irradiation aging versus precipitate dissolution during neutron irradiation. Both processes were observed to occur, with the dominant mechanism being strongly dependent on the initial particle size distribution. Small clusters and large precipitates underwent enhanced aging during irradiation. Intermediate-sized precipitates were susceptible to dissolution, and were probably broken into small Fe clusters by displacement cascades.

Woolhouse and Ipohorski⁽⁴⁸⁾ observed coherency loss in Cu-Fe alloys by TEM methods during a 450 keV HVEM irradiation and a neutron irradiation.

Partial or total coherency loss was observed for all particles greater than about 14 nm diameter. Knoll⁽⁷⁾ found that 14-MeV Cu ion irradiation at 350-500°C of aged Cu-Fe caused loss of precipitate coherency, with results similar to his TEM observations of irradiated Cu-Co. No significant solute segregation to the foil surface was detected from Auger spectroscopy measurements. Takeyama et al.^(10,11,55) irradiated quenched supersaturated Cu-Fe samples in a 650 keV HVEM. Precipitation was observed near the foil surface and the Fe solute segregated to void surfaces during a 10 dpa irradiation at 300°C. Iron enrichment at grain boundaries and near voids was detected from EDS measurements. They concluded that an interstitial-solute interaction was the source of the observed solute segregation.

II.H. Cu-Ge

Saka⁽⁵⁶⁾ has recently studied solute segregation in Cu-5.3 at % Ge during a 1-MeV HVEM irradiation at temperatures from 300-700 K. Radiation-induced segregation was indirectly studied by examining the dissociation width of extended dislocations using weak-beam electron microscopy. The width of extended dislocations was observed to increase dramatically at about 600 K. At higher irradiation temperatures it decreased and approached the room-temperature value. Saka concluded that the increased width implies segregation of the oversized Ge solute toward the dislocation sink. He proposed that a vacancy-solute mechanism was operating due to a large vacancy binding energy, and that the Ge solute was dragged towards sinks by the vacancies. An alternative explanation of the observed segregation phenomena was interstitial-induced inverse Kirkendall effect.

II.I. Cu-In

Rivaud et al.⁽⁵⁷⁾ have investigated the phase stability of Cu-In following a low-energy (< 3 keV) Ar^+ ion irradiation. Enhanced diffusion and solute segregation toward the surface, and radiation-enhanced precipitation (REP) was observed in the irradiated region by using SEM and Auger techniques. The matrix concentration of In at the surface was observed to decrease during irradiation due to preferential sputtering of the In solute. Radiation-enhanced surface segregation partially compensated for the loss of In due to sputtering. A high concentration of In was observed in the irradiated region, indicating that the solute had saturated all of the available sinks. The width of the compositionally altered layer was on the order of the ion penetration range.

II.J. Cu-Mn

Zinkle and Kulcinski⁽¹⁵⁾ monitored the electrical resistivity change of Cu-5% Mn during a room temperature irradiation with 14-MeV neutrons. The electrical resistivity initially decreased, then reached a minimum with increasing dose. The final neutron fluence was not sufficiently high to determine if the resistivity was beginning to increase with dose following the minimum in resistivity. The initial decrease in resistivity was attributed to short range ordering. Macht et al.^(41,42) have used SIMS techniques to determine the partial diffusion coefficient of Cu-Mn following irradiation with 300 keV Cu^+ ions. It was concluded that at temperatures above 450 K the dominant Mn solute diffusion mechanism is via vacancies. At lower temperatures, solute diffusion may take place via weakly bound complexes such as Mn-interstitial or Mn-divacancy.

II.K. Cu-Ni

The Cu-Ni system is single phase for all compositions, and shows complete miscibility in the solid state at temperatures where thermal diffusion is high enough for an observable mass transport. Schüle et al.⁽⁵⁸⁾ used electrical resistivity methods to study the behavior of Cu-Ni alloys during neutron irradiation at temperatures between 100 and 150°C. The resistivity decreased with increasing fluence. This observation was attributed to phase decomposition due to diffusion of irradiation-produced interstitials (interstitialcy mechanism). The interstitial migration energy for Cu-55% Ni was found to be 1.1 eV.

Poerschke and Wollenberger⁽⁵⁹⁻⁶³⁾ have carried out extensive studies of the Cu-Ni system, utilizing resistivity, neutron diffraction, and positron annihilation techniques to investigate the irradiated alloy behavior. Irradiation of Cu-Ni with 3-MeV electrons at temperatures above 100 K caused decreases in the resistivity which were attributed to decomposition of the solid solution by nickel clustering.^(59,63) Arguments were given to show that the clustering is due to an irradiation-induced interstitialcy mechanism. Isochronal annealing and positron annihilation measurements following low-temperature electron irradiation indicated that atomic clustering between 100 K and 250 K is due to interstitial migration. Vacancy migration and vacancy cluster formation occurred at 200-300 K and above.⁽⁶³⁾ In addition to the short range clustering which is observed after low-temperature electron irradiations, a periodic long-range ordering of the short-range ordered clusters has recently been observed following electron irradiation at temperatures between 100 and 200°C.⁽⁶⁵⁾ This long-range structure was found to be stable against thermal annealing and irradiation, and may be an indication of radi-

ation-induced precipitation (RIP). Barlow⁽¹¹⁹⁾ had previously proposed that G.P. zone formation may occur during HVEM irradiation of Cu-Ni at elevated temperatures.

There have been several investigations of surface segregation in Cu-Ni alloys during low-energy ion irradiation. Swartzfager et al.⁽⁶⁶⁾ and Shimizu et al.^(67,68) have measured radiation-enhanced diffusion coefficients for Cu-Ni following low-energy (2-3 keV) Ne and Ar ion bombardment, respectively. The near surface region was found to be Ni rich compared to the bulk for high dose rates. The width of the segregation zone was found to be as large as 1 μm at 873 K along grain boundaries.⁽⁶⁷⁾ At low dose rates, Shimizu et al.⁽⁶⁸⁾ reported that the near surface region was Cu-rich, with a large Cu-depleted zone present underneath it. Their diffusion energy measurements suggested that the surface segregation was caused by an interstitial-type diffusion mechanism.

Rehn et al.⁽⁶⁹⁾ have recently shown that point defect fluxes induced during a 2.2-MeV Ar^+ ion irradiation can cause segregation of Ni toward the surface of initially homogeneous Ni-Cu alloys. An analysis using AES combined with sputtering showed a Ni-enriched surface region and a Ni-depleted region at intermediate depths. The segregation region extended beyond the displacement damage region by ~ 30 nm. A post-irradiation anneal significantly reduced the amount of segregation, indicating that it was radiation-induced as opposed to radiation-enhanced. They concluded that the observed RIS could be explained either by a "size effect" mechanism or an inverse Kirkendall mechanism (fast migration of the slightly over-sized Cu away from sinks via vacancy diffusion). Lam and Wiedersich⁽⁷⁰⁾ have recently developed a comprehensive kinetic model which is in good agreement with experimental observations.

Takahashi et al.⁽¹¹⁾ observed Ni segregation to grain boundaries and voids following a 10 dpa irradiation of Cu-2% Ni at 523-673 K in a 650 keV HVEM. Segregation was attributed to an interaction with interstitials. The segregation of Ni on the voids apparently introduced a spherically coherent strain.⁽⁷⁶⁾ Takeyama⁽⁷¹⁾ noted that the Cu-depleted zone which was observed at grain boundaries following electron irradiation was in agreement with size-effect considerations.

Chountas et al.⁽⁷²⁾ studied the electrical resistivity of neutron-irradiated Cu-50% Ni alloys at irradiation temperatures of 100-300°C. They found that the resistivity decreased with increasing dose. This was attributed to the creation of Ni-rich domains due to radiation-enhanced diffusion. A study of temperature effects found that the resistivity initially decreased with increasing irradiation temperature, and reached a minimum at a temperature of 180°C. The authors attributed this effect to the onset of vacancy migration. Zinkle and Kulcinski⁽¹⁵⁾ have similarly monitored the electrical resistivity of Cu-5% Ni during a room temperature 14-MeV neutron irradiation. The alloy resistivity decreased, reached a minimum, then increased with fluence in a manner similar to what was observed in Cu-5% Al.

Shalaev⁽⁷³⁾ used electrical resistivity measurements to obtain radiation-enhanced diffusion coefficients of neutron-irradiated Cu-Ni alloys for the temperature range 400-700°C. Macht et al.^(41,42) have recently employed SIMS techniques after irradiation with 300 keV Cu⁺ ions at temperatures between 300 and 700 K in order to obtain the partial diffusion coefficient for Cu-Ni. No indication of diffusion via solute-defect complex formation was found (negligible interstitial-solute binding). In addition, vacancy diffusion was claimed to be unimportant. This led to a conclusion that diffusion of Ni in

Cu under irradiation must be by an interstitialcy mechanism (since Cu and Ni are of similar size), in agreement with previous proposals.

II.L. Cu-Pd

There have been several investigations of radiation-induced ordering in Cu-Pd alloys. The following study appears to be the most comprehensive investigation to date. Zee et al.^(21,74) have recently investigated the effect of low-temperature 1.8-MeV electron and 14-MeV neutron irradiation on order-disorder transformations in Cu-Pd along with higher-temperature ion irradiation. Ordered and disordered samples were irradiated, and the results were compared to theoretical predictions. A comparison with other irradiation studies of ordered alloys determined that the difference in atomic size between the solute and solvent is the main factor controlling the amount of reordering by interstitials (larger size difference results in smaller reordering). Electron irradiation was found to be much more effective in reordering than neutron irradiation.

II.M. Cu-Si

Saka⁽⁵⁶⁾ used weak-beam electron microscopy to study RIS in Cu-5.1 at % Si. The dissociation width of extended dislocations was found to increase upon irradiation at temperatures near 600 K, which implies segregation of the oversized Si solute toward the dislocations. Saka suggested that this effect was due to the formation of a vacancy-solute complex, which would lead to solute being dragged toward the sinks along with the vacancies. Takeyama⁽⁷⁵⁾ has recently reported on the effect of 650-keV electron irradiation on the phase stability of Cu-2% Si. Radiation-induced precipitation occurred during irradiation to 10 dpa at 150-300°C. Depletion of Si occurred at grain bound-

aries. The vacancy migration energy of the alloy was found to be larger than that in pure Cu, and a Si-vacancy binding energy of 0.24 eV was estimated.

II.N. Cu-Ti

Hillairet et al.⁽⁷⁶⁾ have irradiated amorphous $\text{Cu}_{50}\text{Ti}_{50}$ specimens with 2.5-MeV electrons to a dose of $1 \times 10^{22} \text{ e/m}^2$. A slight increase in resistivity was observed following the irradiation at 20 K. This excess resistivity annealed out between 20 K and 250 K with no clearly defined recovery stages. At higher annealing temperatures, the resistivity increased and became comparable to the value for nonirradiated specimens. It was determined that no significant short range ordering occurred for these irradiation conditions.

II.O. Cu-Zn

Schüle and coworkers used resistivity methods to investigate radiation-enhanced diffusion in Cu-36% Zn following neutron⁽⁷⁷⁾ and electron⁽⁷⁸⁾ irradiation. The diffusion rate decreased during extended irradiation, becoming nearly temperature independent and was found to depend only on interstitials for irradiation temperatures 50-150°C (interstitialcy diffusion). The degree of short-range order increased during irradiation. The binding energy between interstitials and traps was estimated to be $\sim 0.1 \text{ eV}$.⁽⁷⁸⁾

Takamura and Okuda⁽⁷⁹⁾ studied order-disorder transformations in Cu-Zn (β -brass) following a low temperature fast neutron irradiation by resistivity methods. They assigned the observed annealing for temperatures up to 200 K (60% recovery) to reordering produced by interstitial migration. Poerschke and Wollenberger⁽⁸⁰⁾ measured the electrical resistivity of Cu-Zn (α -brass) during 0.4-3.0 MeV electron irradiation at temperatures between 30 K and 150 K, along with isochronal annealing up to 360 K. Isothermal irradiation or isochronal annealing above 100 K produced negative resistivity changes due to

an increase in short range order. This indicated atomic ordering was occurring via an interstitial mechanism, due to the low temperatures involved. It was found that the observed ordering kinetics of Cu-Zn could be consistently interpreted by interstitialcy diffusion, in contrast to an earlier conclusion by Damask.⁽⁸¹⁾

II.P. Cu-Zr

Hillairet et al.⁽⁷⁶⁾ used resistivity measurements to investigate the effect of a low-temperature ($\lesssim 20$ K) 2.5-MeV electron irradiation on amorphous Cu-Zr alloys. No significant increase in the ordering rate (above that of thermal ordering) was detected for electron fluences up to $1 \times 10^{22}/\text{m}^2$ for a $\text{Cu}_{40}\text{Zr}_{60}$ alloy. Results obtained from a $\text{Cu}_{60}\text{Zr}_{40}$ alloy were found to depend on the thermal history of the specimens. As-quenched $\text{Cu}_{60}\text{Zr}_{40}$ specimens behaved similar to $\text{Cu}_{40}\text{Zr}_{60}$, while specimens which had been aged at room temperature for 1 month exhibited signs of radiation-enhanced ordering.

TABLE 1. Solute Segregation and Phase Stability Experiments on Irradiated Copper Alloys

Solute	Atomic Misfit (%)*	Irradiating Species	Dose**	Irradiation Temperature	Comments	Ref.
Ag 2 at %	+ 43.5	electron	10 dpa (K=0.8)	250°C	Radiation - enhanced precipitation near grain boundaries and foil surface. Depleted solute at voids and grain boundaries.	9,10
Al 1-15 at %	+ 20.0	fast neutron	to 4×10^{22} n/m ² ($\sim 10^{-3}$ dpa, K=0.3)	- 120, 35°C	short range ordering (SRO) implied	12
15 at %		fast neutron	to 3×10^{21} n/m ² ($\sim 10^{-4}$ dpa, K=0.3)	45-250°C	enhancement of thermal aging rate	13
15 at %		neutron (E > 0.1 MeV)	to 1×10^{20} n/m ² ($\sim 3 \times 10^{-6}$ dpa, K=0.3)	13 K	SRO	14
5 at %		14-MeV neutron	to 3×10^{21} n/m ² (4×10^{-4} dpa, K=0.3)	20°C	SRO (?)	15
9 at %		neutron	-	1-4 K	solute seg. around dislocations implied	17
Au 10-25 at %	+ 47.6	2-MeV electron, fast neutron	10^{22} e/m ² , 4.6×10^{20} n/m ² ($\sim 10^{-3}$ dpa, K=0.3)	60-200°C	Radiation-enhanced diffusion (vacancy-type + interstitialcy-type with increasing order).	18
25 at %		neutron, ion, electron	to 10^{-3} dpa (K=0.3)	4-400 K	Radiation-induced order-disorder phase transformation.	19-25
0-2.5 at %		neutron	-	-	Deviation from Matthiessen's Rule	26

TABLE 1. Solute Segregation and Phase Stability Experiments on Irradiated Copper Alloys
(Continued)

Solute	Atomic Misfit (%)*	Irradiating Species	Dose**	Irradiation Temperature	Comments	Ref.
Be	- 26.4					
13.5 at %		fast neutron	to 3×10^{23} n/m ² (~ 0.01 dpa, K=0.3)	0-40°C	Radiation-induced precipitation (RIP) inferred from resistivity, hardness.	27
2.5%		2.5-MeV electron	to 9×10^{20} e/m ² ($\sim 10^{-5}$ dpa, K=0.8)	20°C	Resistivity increase (precipitation) - interstitial mechanism.	28
9.5-13 at %; also ternaries		fast neutron	to 2×10^{23} n/m ² ($\sim 10^{-3}$ dpa, K=0.3)	20-160°C	Enhanced formation of G.P. zones and intermediate γ' phase. In ternary alloys, Mg, Zn accelerate pptn; Co, Fe retard pptn.	29-32
to 0.018 at %		3-MeV electron	to 1×10^{24} e/m ² ($\sim 10^{-2}$ dpa, K=0.8)	5-140°C	Be segregation to internal sinks (interstitialcy migration). One Be atom removed from solid solution for 2-4 Frenkel pairs created.	34,35
3.4 at %		14-MeV Cu	0.1-15 dpa (K=0.3)	300-475°C	Be segregation to surface. Little seg. in damage region due to high sink density. RIP of γ'/γ phase in damage region. Pptn. confined to peak damage region for high temperature irradiations. Ppt-free zones occasionally observed at grain boundaries.	6, 36
1.35 at %		300-keV Cu	0.5-4 dpa (K=0.4)	325-400°C	Uniform RIP of equilibrium γ phase at all doses (Be-interstitial segregation). Some evidence for ppt. dissolution via athermal cascade mixing.	38

TABLE 1. Solute Segregation and Phase Stability Experiments on Irradiated Copper Alloys
(Continued)

Solute	Atomic Misfit (%)*	Irradiating Species	Dose**	Irradiation Temperature	Comments	Ref.
1.35 at %		1-MeV electron	to 1.8×10^{26} e/m ² (0.2 dpa, K=0.8)	325-425°C	RIP of γ'' , γ' phases	39
1.35 at %		300-keV Cu	0.1-8 dpa (K=0.4)	25-425°C	RIP of γ phase observed for 225-425°C. Be segregation out of damage region (interstitial-solute complex).	40-42
1.3, 6.1%		650-keV electron	to 5×10^{25} e/m ²	280-430°C	Accelerated formation of intermediate phases (Be-interstitial migration).	43
Co 2 %	- 3.78	fission neutron	3.4×10^{23} n/m ² (~ 0.01 dpa, K=0.3)	50°C	Decreased density of particles \leq 2.5 nm diameter. Ppt. density increased and particle size decreased for specimens containing larger particles.	44
1 %		neutron (E > 1 MeV)	$0.5-1.5 \times 10^{23}$ n/m ² (< 0.01 dpa, K=0.3)	40-210°C	Increased precipitation compared to control samples. Irradiated ppt. size roughly constant with temp. while control ppt. size varied by a factor of two.	45
1 at %		14-MeV Cu	0.3-1.7 dpa, (K=0.3)	400-475°C	Precipitate-matrix interface becomes incoherent.	7
1-2.65%		450-keV electron; fast neutron	to 1×10^{26} e/m ² ; $0.1-1.6 \times 10^{22}$ n/m ² ($< 10^{-3}$ dpa, K=0.3)	20-100°C	Larger precipitates become incoherent. Loss of coherency due to interaction with interstitial loops or free interstitials.	46-48

TABLE 1. Solute Segregation and Phase Stability Experiments on Irradiated Copper Alloys
(Continued)

Solute	Atomic Misfit (%)*	Irradiating Species	Dose**	Irradiation Temperature	Comments	Ref.
Cr 0.3%	+ 19.7	laser	-	ambient	Precipitate dissolution	49
Fe 2.4%	+ 4.57	0.5-MeV electron 9-MeV proton	-	20°C	Accelerated precipitation kinetics; protons cause ppt. dissolution.	50,51
0.8-5.0%		neutron (E > 0.25 MeV)	to 2×10^{24} n/m ² (< 0.1 dpa, K=0.3)	60-70°C	Precipitate dissolution, RIP inferred from resistivity. Either radiation-enhanced aging or ppt. dissolution occurs depending on preirrad. treatment.	52,53
0.6 at %		neutron (E > 0.1 MeV)	$0.4-9 \times 10^{23}$ n/m ² (\geq 0.01 dpa, K=0.3)	55°C	Coarsening of small, large ppts; dissolution of intermediate-sized ppts. Very small Fe cluster formation due to enhanced diffusion.	54
1%		450-keV electron fast neutron	to 1×10^{26} e/m ² , $0.1-1.6 \times 10^{22}$ n/m ² ($< 10^{-3}$ dpa, K=0.3)	20°C	Precipitate-matrix interface becomes incoherent.	48
1 at %		14-MeV Cu	1-5 dpa (K=0.3)	350-500°C	Precipitates lose coherency. No evidence of Fe segregation to the surface.	7
2 at %		650-keV electron	to 10 dpa (K=0.8)	250, 300°C	Fe segregation to voids, grain boundaries.	10, 11,55

TABLE 1. Solute Segregation and Phase Stability Experiments on Irradiated Copper Alloys
(Continued)

Solute	Atomic Misfit (%)*	Irradiating Species	Dose**	Irradiation Temperature	Comments	Ref.
Ge 5.3 at %	+ 27.8	1-MeV electron	$1 \times 10^{26} \text{ e/m}^2$	25-425°C	RIS of Ge to dislocations implied from dissociation width of extended dislocations.	56
In 3,10 at %	+ 79.0	1-3 keV Ar	2.6 dpa (K=0.8)	30-385°C	REP observed. Solute segregation toward the surface.	57
Mn 5 at % "sandwich alloy"	+ 34.2	14-MeV neutron 300-keV Cu	to $3 \times 10^{21} \text{ n/m}^2$ ($4 \times 10^{-4} \text{ dpa}$, K=0.3) -	20°C 25-425°C	short range ordering (?) Mn diffuses via vacancies above 175°C. Lower temp. diffusion via weakly bound complexes.	15 41,42
Ni 35-85% 42-71 at %	- 8.45	fast neutron 3-MeV electron	to $1 \times 10^{22} \text{ n/m}^2$ ($< 10^{-3} \text{ dpa}$, K=0.3) to $8 \times 10^{22} \text{ e/m}^2$	100-150°C 4 K - 325°C	Decomposition of single phase (interstitialcy diffusion). Decomposition of single phase for irradiation above 100 K (interstitialcy mechanism). (59,63) Interstitialcy diffusion dominant below 250 K. (63)	58 59-63

TABLE 1. Solute Segregation and Phase Stability Experiments on Irradiated Copper Alloys
(Continued)

Solute	Atomic Misfit (%)*	Irradiating Species	Dose**	Irradiation Temperature	Comments	Ref.
59 %		3-MeV electron	to 6×10^{23} e/m ²	100-370°C	Possible RIP for irradiation between 100-200°C.	65
9-50 at %		2-keV Ne, 3-keV Ar	-	25-600°C	Radiation-enhanced diffusion (interstitial-type). Ni segregation to surface and grain boundaries; Cu-rich surface region for low dose rates (2.5×10^{16} /m ² -s) at 600°C(68).	66-68
40, 90 at %		2.2-keV ion	5 dpa (K=0.8)	500, 515°C	RIS of Ni to surface	69
2 at %		650-keV electron	7-10 dpa (K=0.8)	250-400°C	Ni segregation to grain boundaries and voids.	11,71
50 at %		fast neutron	3.6×10^{21} n/m ² ($\sim 10^{-4}$ dpa, K=0.3)	100-300°C	Formation of Ni-rich clusters implied.	72
5 at %		14-MeV neutron	to 3×10^{21} n/m ² (4×10^{-4} dpa, K=0.3)	20°C	SRO (?)	15
"sandwich alloy"		300-keV Cu, neutron(73)	- -	80 K - 425°C 400-700°C	Diffusion coefficients measured for different damage rates (interstitialcy mechanism).	41,42 73
Pd	+ 28.0	14-MeV Cu 1.8-MeV electron 14-MeV neutron	0.02-2 dpa (K=0.3) 3×10^{-4} dpa (K=0.8) $\sim 1 \times 10^{-4}$ (K=0.3)	20-550°C 100 K 4 K	Radiation-induced ordering; electrons more effective. Ion irradiation gave disordering at low temp., reordering at high temp.	21,74

TABLE 1. Solute Segregation and Phase Stability Experiments on Irradiated Copper Alloys
(Continued)

Solute	Atomic Misfit (%)*	Irradiating Species	Dose**	Irradiation Temperature	Comments	Ref.
Si	+ 5.08					
5.1 at %		1-MeV electron	1×10^{26} e/m ²	25-425°C	RIS of Si to dislocations at higher temperatures.	56
2%		650-keV electron	10 dpa (K=0.8)	150-300°C	RIP observed. Si depleted at grain boundaries. Si-vacancy binding energy ~ 0.24 eV.	75
Ti	+ 25.7					
50%		2.5-MeV electron	1×10^{22} e/m ²	20 K	no significant short range ordering	76
Zn	+ 17.1					
20-36%		neutron (E > 1 MeV)	-	40-150°C	SRO observed (interstitialcy diffusion); interstitial-trap energy ~ 0.1 eV.	77,78
		2-MeV electron	2×10^{22} e/m ²			
25,48%		neutron (E > 0.1 MeV)	3×10^{20} n/m ² (~ 10^{-5} dpa, K=0.3)	4.2 K	Ordering due to interstitial migration; vacancy ordering above 200 K.	79
20-36 at %		0.4-3 MeV electron	to 1×10^{23} e/m ² ($\leq 10^{-3}$ dpa, K=0.8)	30-150 K	SRO (interstitialcy mechanism)	80
Zr	-					
40,60%		2.5-MeV electron	1×10^{22} e/m ²	20 K	Possible radiation-enhanced ordering in Cu ₆₀ Zr ₄₀	76

* Volume size-factors from King⁽⁹⁾ in percent. A positive value denotes oversized solute.

** Neutron damage level estimated using dpa-fluence correlations (see introduction). Damage levels for ion and electron irradiations (when given) are from the original papers -- no dpa-fluence correlations were attempted for these particles.

III. Void and Loop Studies

Copper is susceptible to void formation when irradiated to doses on the order of a fraction of a dpa at temperatures between 200 and 550°C. Much of the work on radiation-induced void and loop formation was performed in the late 1960's and early 1970's. Comprehensive reviews of loop formation in irradiated copper have been presented by Rühle,⁽⁸²⁾ Wilkens,⁽⁸³⁾ and Eyre.⁽⁸⁴⁾ Knoll⁽³⁾ recently updated these reviews and summarized the published TEM studies on irradiated copper/copper alloys.

III.A. Neutron Irradiations

To date, there is no known systematic neutron irradiation study which has comprehensively investigated the combined effects of temperature, fluence, dose rate, or transmutation products on void swelling in copper. The results of all known void swelling studies of neutron irradiated copper and copper alloys are given in Table 2.

III.A.1. Pure Copper Void Formation Due to Neutron Irradiation

Copper has been found to contain voids when irradiated with neutrons at temperatures between 220 and 550°C ($0.35-0.60 T_{mp}$).⁽⁸⁵⁻⁹⁶⁾ Void formation in high purity copper has been investigated for relatively modest fast neutron fluences ranging from $1 \times 10^{21} \text{ n/m}^2$ to $1.3 \times 10^{26} \text{ n/m}^2$ ($\lesssim 10^{-4} - 4 \text{ dpa}$, $K = 0.3$). The maximum reported amount of void swelling in copper following fast neutron irradiation is 0.51%.⁽⁹²⁾ This occurred following irradiation to a fluence of $4.1 \times 10^{24} \text{ n/m}^2$ ($\sim 0.2 \text{ dpa}$, $K = 0.3$) at a temperature of 327°C.

In high purity copper, the variation of void swelling with temperature for neutron irradiation is similar to that in many other pure metals. Swelling occurs at intermediate temperatures of about $0.35 T_{mp}$ to $0.57 T_{mp}$, with a broad peak situated near the middle of this range. Voids were observed in

copper irradiated to a dose of $5 \times 10^{24}/\text{m}^2$ (0.14 dpa, $K = 0.3$) by Levy et al.,⁽⁸⁶⁾ Adda,⁽⁸⁷⁾ and Labbe et al.^(90,91) at temperatures of 220°C to 500°C. Peak swelling of about 0.40% occurred at $\sim 340^\circ\text{C}$.⁽⁹¹⁾ The mean void diameter increased from ~ 5 nm to more than 150 nm over this temperature range, while void concentration decreased rapidly from a maximum of $4 \times 10^{20}/\text{m}^3$, showing that higher temperature inhibits nucleation but favors growth. Labbe and co-workers^(90,91) investigated the effect of a lower dose rate in shifting the swelling maximum to lower temperatures. The peak swelling temperature was reduced 20°C in specimens that were irradiated to the same fluence as above, but at a dose-rate ten times lower.⁽⁹¹⁾ The voids observed here and in other work^(85,89) were octahedra bounded by $\{111\}$ planes, often truncated at the corners.

The dependence of void nucleation and growth on neutron fluence was studied by Brimhall and Kissinger⁽⁸⁹⁾ at a temperature of 285°C. No threshold fluence for swelling was observed, although a plot of swelling vs. fluence suggested a threshold at doses lower than $\sim 5 \times 10^{22}$ n/m². Void nucleation continued up to doses of at least 1.2×10^{24} n/m², but the void density began to saturate at fluences above $\sim 3 \times 10^{23}$ n/m². Below this fluence the void density increased approximately linearly with dose. The threshold fluence for neutron swelling has been found to be less than 10^{21} n/m² ($\sim 4 \times 10^{-5}$ dpa, $K = 0.3$) by Muncie.^(93,94)

Several interesting observations of the relation between dislocation structure and void formation during neutron irradiation have been made. Brimhall and Kissinger⁽⁸⁹⁾ noted that voids nucleated concurrently with dislocation loops, but not subsequent to loop formation. The dislocation structure, which consisted of loops and tangles, increased in density as fluence

increased, then saturated at the same dose where void nucleation ceased. There was no spatial correlation between voids and dislocations. When dislocations were introduced by pre-irradiation cold-working of specimens,^(87,90) there appeared to be an optimum dislocation density for swelling. Slightly cold-worked specimens irradiated at 250°C swelled more than annealed specimens but heavily cold-worked specimens swelled less. Adamson et al.⁽⁹²⁾ observed significant denudation of voids and dislocations at grain and twin boundaries in copper irradiated at 327°C to a fluence of $4 \times 10^{24} \text{ n/m}^2$ ($\sim 0.2 \text{ dpa}$, $K = 0.3$).

Eldrup et al.⁽⁹⁵⁾ used positron annihilation techniques along with TEM to investigate void formation in Cu irradiated at 250°C to a fluence of $5 \times 10^{22} \text{ n/m}^2$ ($\sim 10^{-3} \text{ dpa}$, $K = 0.3$). The average void size was found to be $\sim 15 \text{ nm}$. The voids annealed out at a temperature of 450–500°C. English⁽⁹⁴⁾ reported void formation in neutron-irradiated copper for temperatures 250–350°C. A bimodal size distribution was observed in samples irradiated at 300 and 350°C. Voids were detected at fluences as low as $1 \times 10^{21} \text{ n/m}^2$ ($\lesssim 10^{-4} \text{ dpa}$) for specimens irradiated at 250 and 300°C. Yoshida et al.⁽⁹⁶⁾ have tentatively reported void formation in copper following a 400°C 14-MeV neutron irradiation to a fluence of 10^{22} n/m^2 .

III.A.2. Copper Alloy Void Formation Due to Neutron Irradiation

Only a few studies have been reported concerning void formation in copper alloys following neutron irradiation. Substantial void suppression has been observed in Cu-Al, Cu-Si and Cu-Ge alloys irradiated at 220–350°C.^(87,90) This result was attributed to a lower stacking fault energy in these alloys, which theoretically makes void formation less favorable. On the other hand, Wolfenden⁽⁸⁸⁾ observed a low density of large voids in Cu-10% Al following a

high-fluence irradiation at a temperature of 175°C, where void formation does not occur in pure copper. This result was proposed to be due to the higher vacancy mobility in the alloy as compared to pure Cu, which would allow void nucleation to occur at lower temperatures.⁽⁸⁷⁾ Brimhall and Kissinger⁽⁸⁹⁾ found that Cu-Ni alloys were very resistant to void formation. This suppression was attributed to interstitial trapping by the Ni, since the alloy has a stacking fault energy similar to pure copper. There have been several studies of void formation in neutron-irradiated Cu-Ge alloys.^(87,90,94) Irradiation at 250°C caused 0.1% swelling for 1 and 2.5 wt.% Ge, while measurable swelling did not occur in 3-5% Ge alloys, which have a lower SF energy.^(87,90) English⁽⁹⁴⁾ reported that Cu-Ge alloys exhibited substantial void swelling suppression for temperatures of 250-350°C, with the void volume fraction decreasing with increasing alloy content at all temperatures. The radiation damage was observed to be heterogeneously distributed in both the alloys and in pure copper. The reduction of void swelling with alloy content was due to a large decrease in the void concentration. The cause of this observation was not discussed.

III.A.3. Pure Copper Loop Formation Due to Neutron Irradiation

Copper irradiated with neutrons in the temperature range 20-200°C has been observed to form dislocation tangles, defect clusters, and vacancy and interstitial loops which are predominantly formed on {111} planes.⁽⁹⁷⁻¹⁰⁷⁾ Narayan and Ohr⁽¹⁰⁴⁾ also observed perfect loops ($b = a/2 [110]$) following fusion and fast neutron irradiation. The observed dislocation loops have ranged in size from 1.0 nm to ~ 50 nm, with overall densities of $10^{21}/\text{m}^3$ - $10^{23}/\text{m}^3$. There are indications that the smaller loops tend to be vacancy-type while the larger loops are interstitial.^(84,90,94,98) There continues to be

considerable disagreement regarding the relative proportion of vacancy and interstitial loops, with various groups reporting the visible loop distributions to be either predominantly interstitial or predominantly vacancy.⁽⁸⁴⁾ Several recent TEM studies have reported that most of the visible loops are either vacancy,⁽⁹⁴⁾ interstitial,⁽¹⁰⁴⁾ or roughly equal vacancy and interstitial.⁽¹⁰⁵⁾ Ghoniem et al.⁽¹⁰⁶⁾ have recently shown theoretically that the relative proportion of vacancy versus interstitial loops varies strongly with fluence, indicating that fluence differences may be the source of the observed discrepancies.

Brager et al.⁽¹⁰⁷⁾ recently used TEM to observe defect clusters in copper irradiated with 14-MeV neutrons at room temperature. They reported that the visible defect cluster density increased directly with neutron fluence. Both vacancy and interstitial clusters were identified, with Burgers vectors of $a/2 \langle 110 \rangle$ and $a/2 \langle 111 \rangle$. A survey of the reported loop size distribution data in the literature reveals that the curves can generally be fitted by a log-normal (skewed Gaussian) distribution. Previous analyses have attempted to use the relation $N(d) = N_0 \exp(-d/d_0)$ to describe the loop diameter (d) distribution.^(84,98,111) It has been found⁽¹⁵⁾ that good agreement between observed TEM data and resistivity and microhardness data could only be obtained by using a log-normal size distribution, as opposed to the alternative size distribution mentioned above. Yoshida et al.⁽⁹⁶⁾ have recently reported on loop formation on copper following a 14-MeV neutron irradiation to 1×10^{22} n/m² ($\sim 1 \times 10^{-3}$ dpa, $K = 0.3$). Both stacking fault tetrahedra and dislocation loops were observed for irradiation temperatures below 400°C. The dislocation loop density increased nearly linearly with fluence with 80% of them interstitial-type, and a higher loop density was observed along dislocation lines as opposed to in the matrix.

Conflicting results regarding the effect of neutron energy on loop formation have been reported. Mitchell et al.^(100,105) reported that fusion neutrons were roughly 10 times more effective than fast neutrons with regard to radiation strengthening and defect cluster formation for a room temperature irradiation. Conversely, other researchers^(104,109) have observed only a factor of three difference in the cluster densities for copper irradiated with fission versus D-Be or DT neutrons. Narayan and Ohr⁽¹⁰⁴⁾ found that the nature of defect clusters in irradiated copper was similar for fusion and fast neutron irradiations. Howell⁽¹¹²⁾ determined from positron annihilation measurements of 14-MeV neutron irradiated copper that a variation in dose rate of 3 orders of magnitude did not affect cluster formation, at least for fluences up to $5 \times 10^{20} \text{ n/m}^2$.

Annealing studies of copper irradiated near room temperature indicate that interstitial loops become unstable at $\sim 325^\circ\text{C}$, and vacancy clusters or voids form.⁽¹⁰¹⁾ Annealing above 500°C removes all visible damage.⁽¹⁰²⁾ The defect structure resulting from higher temperature irradiations has been found to be quite different from that at room temperature. English⁽⁹⁴⁾ noted that an increase in the neutron irradiation temperature from 80 to 250°C caused the vacancy loop concentration to decrease by two orders of magnitude. In copper exposed to 10^{22} n/m^2 fast neutrons at 400°C , Hulett et al.⁽⁹⁷⁾ found the damage was confined to "defect regions" 10 - $100 \text{ }\mu\text{m}$ in size, separated by apparently perfect crystal. These regions contained dislocation tangles, vacancy clusters $\lesssim 20 \text{ nm}$ diameter (possibly voids), sessile vacancy loops 10 - 50 nm diameter, and large prismatic loops that were predominantly interstitial.

Several researchers have used x-ray diffuse scattering to examine defect cluster formation in copper following neutron irradiation.^(99,108-110) Good

agreement with TEM measurements was obtained for loop sizes larger than about 2.5 nm. V. Guerard and Peisl⁽¹⁰⁸⁾ investigated defect annealing following a 4.6 K neutron irradiation using this technique. Interstitial clusters were found to collapse into loops at 30-40 K and vacancy loops formed at 150 K. The loop size increased with annealing temperature from ~ 90 interstitials/loop at 70 K to ~ 330 interstitials/loop at 300 K.

III.A.4. Copper Alloy Loop Formation Due to Neutron Irradiation

Ipohorski and Brown⁽¹¹³⁾ observed that the addition of Be to copper resulted in a decreased concentration of interstitial loops following neutron irradiation. Brager et al.⁽¹⁰⁷⁾ investigated defect cluster formation in Cu, Cu-5% Al, Cu-5% Mn and Cu-5% Ni following a low-dose 14-MeV neutron room temperature irradiation. They found that the alloys containing Mn and Ni solute had damage microstructures similar to pure copper, while the Cu-Al alloy had roughly twice as high a visible (loop diameter > 1.0 nm) defect cluster density. Both interstitial and vacancy clusters were observed, and the size distribution of the clusters were similar for all four materials. A fast neutron irradiation of Cu-Ge at 80°C produced a homogeneous distribution of small (< 14 nm) dislocation loops.⁽⁹⁴⁾ Most of the loops (90%) were vacancy-type for Cu-0.1% Ge alloys. Increasing the solute concentration to 1% Ge resulted in a doubling of the loop concentration, with 50% of the loops being vacancy-type. Higher temperature irradiation (250-350°C) produced heterogeneously distributed defect clusters whose concentration was found to decrease with increasing alloy content and temperature.

TABLE 2. Void and Selected Dislocation Loop Studies in Neutron Irradiated Copper and Copper-Base Alloys

Specimen Purity*/ Alloy Concent.	Neutron Energy (MeV)	Flux ($10^{17}/m^2-s$)	Fluence ($10^{24}/m^2$)	Dose** (dpa, K=0.3)	Irradiation Temp. (°C)	Defect***	Mean Diameter (nm)	Density ($10^{20}/m^3$)	Swelling $\Delta V/V$ (%)	Comments	Ref.
99.999%	> 1	-	1.2	0.05	260	V	23	3	0.17	Octahedral voids, bounded by {111} planes.	85
99.99%	> 0.1	25	5	0.14	220 250 300 335 435 450 600 250	V V V V V V V V	5 23 - 56 > 150 - - - -	- 3.5 - 0.27 10^{-6} - ~ 0 - -	~ 0 0.16 ~ 0.3 0.32 0.003 ~ 0.02 0 0.31 0.14	Effect of temperature	86, 87
99.99%, light CW 99.99%, as rolled	> 0.1 > 0.1	25 25	5 5	0.14 0.14	250 250	V V	- -	- -	- -	Effect of cold work	
99.999%	> 0.1	-	130	3.8	175	L	-	-	0	Low-temp. limit for voids	88
99.999%	> 1	0.4-0.9	0.055 0.088 0.133 0.160 0.240 1.27	0.002 0.004 0.006 0.007 0.01 0.05	285 285 285 285 285 260	L,V L,V L,V L,V L,V L,V	12 12 15.9 16.8 18.7 29	0.7 1.0 1.2 1.6 2.2 3.2	0.006 0.011 0.024 0.038 0.074 0.38	Effect of fluence	89

TABLE 2. Void and Selected Dislocation Loop Studies in Neutron Irradiated Copper and Copper-Base Alloys
(Continued)

Specimen Purity*/ Alloy Concent.	Neutron Energy (MeV)	Flux ($10^{17}/\text{m}^2\text{-s}$)	Fluence ($10^{24}/\text{m}^2$)	Dose** (dpa, $K=0.3$)	Irradiation Temp. ($^{\circ}\text{C}$)	Defect***	Mean Diameter (nm)	Density ($10^{20}/\text{m}^3$)	Swelling $\Delta V/V$ (%)	Comments	Ref.
99.99%	> 0.1	28	5	0.14	220	V ?	< 5	~ 0	~ 0	Temperature dependence of void swelling at three different dose rates. Swelling peak shifts to lower temperatures by ~ 20°C as neutron flux is decreased by a factor of 10. Octahedral voids bounded by {111} planes.	90
					250	V	27.5	2.2	0.16		
					335	V	67	0.17	0.32		
					435	V	~ 380	0.0008	0.23		
					550	-	-	0	~ 0		
h.p.	> 0.1	8	6.5	0.19	220	L	-	-	-		91
					250	V	18.5	4.3	0.16		
					335	V	57	0.36	0.35		
					435	V	82	0.08	0.25		
					550	-	-	0	0		
					250	V	28.5	1.8	0.23		
					335	V	71	0.2	0.40		
					435	V	~ 165	0.01	0.30		
					550	-	-	0	0		
99.9%	> 1	-	4.1	0.17	327	V	54,85	0.6,0.2	0.51	Higher density of smaller voids in deformed regions.	92
99.999%	0.1	3.5	0.01	3×10^{-4}	250	V	14	-	-	Low dose void formation.	95
	0.1	3.5	0.05	1.4×10^{-3}	250	V	17	0.5-5	-		
99.999%	14	-	0.009	1×10^{-3}	400	V?	-	-	-		96

TABLE 2. Void and Selected Dislocation Loop Studies in Neutron Irradiated Copper and Copper-Base Alloys
(Continued)

Specimen Purity*/ Alloy Concent.	Neutron Energy (MeV)	Flux ($10^{17}/m^2-s$)	Fluence ($10^{24}/m^2$)	Dose** (dpa, K=0.3)	Irradiation Temp. (°C)	Defect***	Mean Diameter (nm)	Density ($10^{20}/m^3$)	Swelling $\Delta V/V$ (%)	Comments	Ref.
99.998%	> 1	-	0.001	4×10^{-5}	80	L	(< 12)	(62)	-	Low dose void formation as a function of temperature and fluence. Bimodal void distribution observed at 300°C and 350°C. (Thesis work by Muncie ⁹³ .)	94
			0.001	4×10^{-5}	250	V, L	2.8	1.2	1.5×10^{-4}		
			0.003	1×10^{-4}	250	V, L	4.1	2	0.001		
			0.009	4×10^{-4}	250	V, L	5.3	3	0.0025		
			0.021	9×10^{-4}	250	V, L	5.0	5	0.0035		
			0.0008	3×10^{-5}	300	V	3.0	0.3	4×10^{-5}		
			0.004	2×10^{-4}	300	V	4.8	0.7	4×10^{-4}		
			0.012	5×10^{-4}	300	V	6.8	0.6	9×10^{-4}		
			0.025	1×10^{-3}	300	V	15.3	0.2	0.0035		
			< 0.02	1×10^{-3}	350	SFT	-	-	0		
			0.021	1×10^{-3}	350	V	-	≤ 0.1	0.001		
Cu-02 Cu-H2	> 0.1	25	5	0.14	250	V	41	0.9	0.28		87
					250	V	61	0.2	0.31		
1% Al 7% Al	> 0.1	25	5	0.14	250	-	-	-	0	Al lowers the stacking fault energy and either suppresses void swelling or shifts it to lower temperatures.	87
					220, 250, 350	-	-	-	0		
1% Al 3% Al 5% Al	> 0.1	30	5	0.14	250	V	-	few	~ 0		90
						-	-	0	0		
						-	-	0	0		
10% Al	> 0.1	-	130	3.8	175	L, V	to 350	$\sim 10^{-3}$	-		88

TABLE 2. Void and Selected Dislocation Loop Studies in Neutron Irradiated Copper and Copper-Base Alloys
(Continued)

Specimen Purity*/ Alloy Concent.	Neutron Energy (MeV)	Flux ($10^{17}/m^2-s$)	Fluence ($10^{24}/m^2$)	Dose** (dpa, $K=0.3$)	Irradiation Temp. (°C)	Defect***	Mean Diameter (nm)	Density ($10^{20}/m^3$)	Swelling $\Delta V/V$ (%)	Comments	Ref.
2.5% Ge 5% Ge	> 0.1	25	5	0.14	250	V	46.5 50	0.2 < 10^{-6}	~ 0.1 ~ 0	Ge lowers the stacking fault energy and suppresses void swelling through a lower void density. Interstitial loop concentration increases with increasing Ge content.	87
1% Ge 3% Ge	> 0.1	30	5	0.14	250	V	48 60	0.025 few	0.1 ~ 0		90
0.01% Ge 0.1% Ge 1%, 5% Ge	> 1	-	0.01	4×10^{-4}	250 300 350 250 300 350 250-350	V, L V, L V, L V, L V, L L L	5.9 9.7 14.1 8.1 11.5 - -	- - - - - - -	- 0.0056 - - - 0 0		94
2% Ni 20% Ni	> 1	0.4-0.9	0.24	0.01	285 285	V -	30 -	0.1 -	0.01 0	Addition of Ni suppresses void swelling.	89
1% Si	> 0.1	30	5	0.14	250	V	12	few	~ 0	Si lowers the stacking fault energy.	90
0.0001 - 1% Be	> 1	1	0.005	2×10^{-4}	40	L	-	-	0	Addition of Be decreases interstitial loop concentration.	113

*All specimens are in the annealed state unless otherwise indicated.

** Damage level calculated assuming: $1 \times 10^{26} \text{ n/m}^2$ ($E > 0.1 \text{ MeV}$) $\approx 2.9 \text{ dpa}$ ($K = 0.3$)

$1 \times 10^{26} \text{ n/m}^2$ ($E > 1 \text{ MeV}$) $\approx 4.2 \text{ dpa}$ ($K = 0.3$)

$1 \times 10^{26} \text{ n/m}^2$ ($E = 14 \text{ MeV}$) $\approx 15 \text{ dpa}$ ($K = 0.3$)

(see introduction section)

*** V = void, L = dislocation loop, SFT = stacking fault tetrahedra

III.B. Electron Irradiations

Details of the known investigations of void and loop formation in copper and its alloys following electron irradiation are given in Table 3.

III.B.1. Pure Copper Void Formation Due to Electron Irradiation

Voids have been observed by several investigators in HVEM-irradiated Cu in the temperature range 250-550°C,^(55,114-125) with the swelling sharply peaked around 450-500°C depending on dose rate. One study also reported void formation for irradiation temperatures of 100-250°C,⁽¹¹⁴⁾ and another investigation found that the peak swelling temperature for copper was 250°C.⁽⁵⁵⁾ (The variance in the observed swelling temperatures may be due to gas effects, to be discussed later in this review.) The maximum known void swelling in HVEM-irradiated copper is 17% at an irradiation temperature of 250°C,⁽¹¹⁴⁾ although higher values may have been achieved.⁽¹¹⁵⁾ High purity copper does not appear to have any appreciable incubation dose for electron irradiations, c.f. Ref. 55. The swelling rate has been found to be $\geq 0.8\%/dpa$ ($K = 0.8$) by Takeyama et al.⁽⁵⁵⁾ Swelling saturation has been observed for doses greater than 75 dpa by Makin.⁽¹¹⁴⁾

The variation of swelling with temperature has been found to be asymmetric with respect to the peak swelling temperature;⁽¹¹⁸⁻¹²⁰⁾ at higher temperatures, swelling decreased abruptly, but below the peak it dropped off more slowly and exhibited a "tail" at low temperatures (Fig. 1). There are indications that the swelling rate increases with irradiation temperature up to a temperature of 450-500°C.^(115,119) Barlow⁽¹¹⁹⁾ found that swelling was linear with dose following an incubation period of 2-10 dpa. He observed a maximum swelling rate of 0.5%/dpa. Leffers et al.⁽¹¹⁵⁾ reported a maximum swelling rate of $\sim 0.6\%/dpa$ at 450°C. The swelling rate was $\leq 0.1\%/dpa$ at

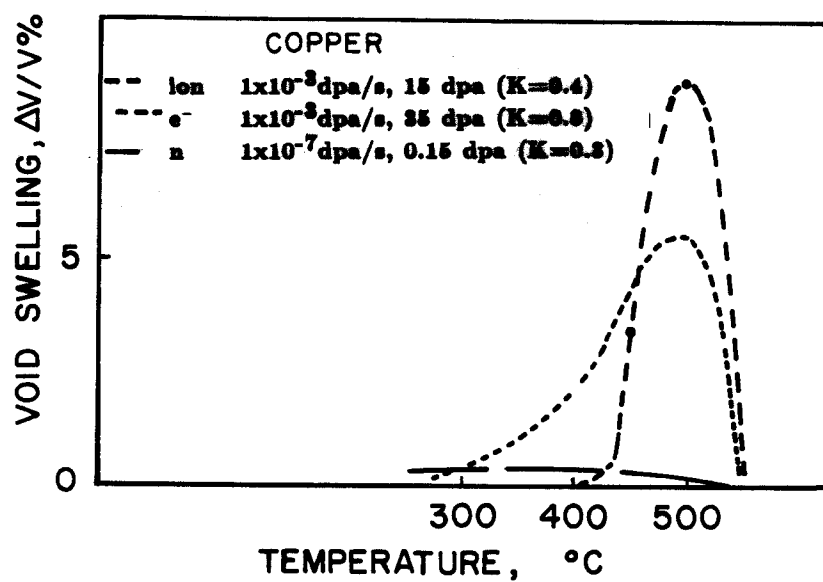


Fig. 1. [Ref. 143] Void swelling vs. temperature in copper irradiated with neutrons, electrons, and copper ions.

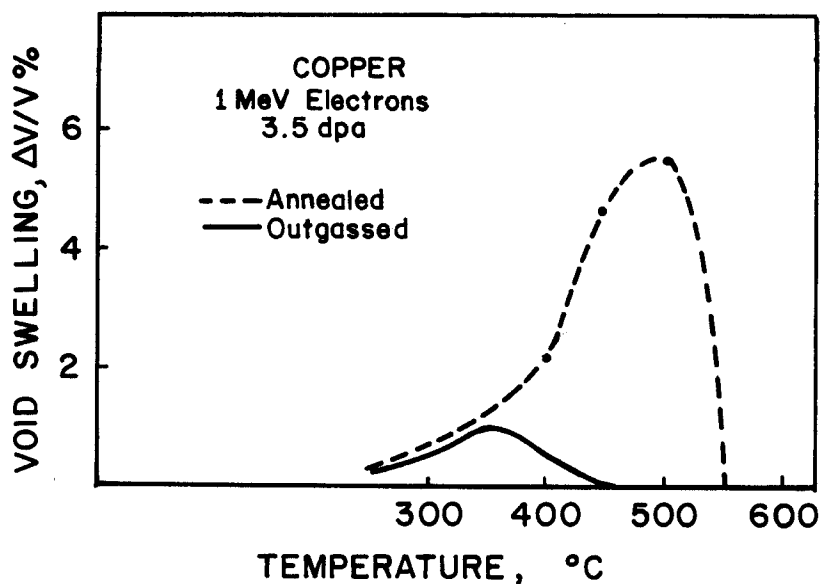


Fig. 2. [Ref. 143] Effect of outgassing on void swelling in copper.

250°C. Barlow⁽¹¹⁹⁾ observed that the void concentration at a given temperature was roughly constant with respect to dose, whereas it varied by a factor of five over the irradiation temperature range of 250° - 450°C.

Makin⁽¹¹⁴⁾ observed that copper injected with argon displayed enhanced void nucleation while retaining the same swelling behavior with dose as pure copper at 250°C. Conversely, copper containing helium bubbles (2000 ppm) did not form voids after 23 dpa at 250°C. The latter behavior was attributed to the bubbles suppressing void formation by acting as efficient point defect sinks. Barlow⁽¹¹⁹⁾ found that preinjected helium enhanced void formation for low injection levels. The void density saturated for He concentrations ≥ 50 appm, depending on the temperature. Glowinski⁽¹¹⁸⁾ found that high purity copper prepared using standard techniques swelled readily, while copper that had been degassed in high vacuum prior to irradiation showed reduced swelling and a shift of the swelling peak to lower temperatures by about 150°C (from 500°C to 360°C). No voids formed in degassed copper specimens irradiated at temperatures above 440°C (Fig. 2). The presence of gas was thought to enhance void nucleation and growth by nucleating interstitial loops and stabilizing dislocation networks that were necessary to achieve a net interstitial bias.

Buckley et al.⁽¹²⁴⁾ investigated the effect of the vacuum surrounding the specimen on void nucleation at temperatures between 250 and 450°C. No effect on void swelling was found while varying the vacuum by several orders of magnitude during irradiation. Previous preliminary results⁽¹²⁵⁾ had suggested that void formation in annealed copper becomes increasingly difficult with better vacuum pressure. In the more current study, they found that the observed suppression of void swelling was caused by use of foils which were too thin. For irradiation temperatures of 250-300°C, a constant high density of

voids was observed in foils above 500 nm thickness, while zero void density was observed in foils of less than 450 nm thickness (independent of vacuum pressure).

Dose rate effects on void swelling in the HVEM apparently depend on specimen purity. Glowinski⁽¹¹⁸⁾ observed a swelling maximum of 500°C in non-degassed copper, and at 345°C in degassed copper specimens which were irradiated at a dose rate of 1.3×10^{-3} dpa/sec. Barlow^(119,120) found that peak swelling occurred at 450°C for a dose rate of 1×10^{-2} dpa/sec.

There have been several investigations on the influence of dislocation structure on void formation.^(114,115,117,118,123) The experimental results are best summarized by the observations of Kenik and Mitchell⁽¹¹⁷⁾: (a) void nucleation (i.e. void density and the dose at which voids appear) is strongly influenced by the initial dislocation density and its subsequent behavior during irradiation; (b) void growth is related to the average dislocation density during irradiation; and (c) above some dislocation density ($2.5 \times 10^{13}/\text{m}^2$ here) dislocation motion is hindered and swelling decreases, indicating that the interstitial bias is reduced. In foils thin enough for most dislocations to escape (< 300 nm), no voids formed at 300°C. In one study⁽¹¹⁴⁾ voids formed only in the vicinity of dislocation walls for irradiation temperatures greater than 350°C. Glowinski⁽¹¹⁸⁾ found that voids formed at temperatures above 300°C only if the specimens were first irradiated at a lower temperature (100°C) to introduce a dislocation structure. Fisher et al.⁽¹²²⁾ observed that void formation was preceded by a rapid buildup of dislocation loops and development of a dislocation network. The void density was found to be linear with dose up to 10 dpa, where saturation set in. The void size increased monotonically with dose. Leffers et al.^(115,123) performed a

comprehensive evaluation of the effect of cold-work (CW) levels ranging from 0 to 90% on void swelling in copper. Swelling was found to initially increase with cold work level, reach a maximum around 50% CW, then decrease at the high cold work levels. The voids were homogeneously distributed at low CW levels and heterogeneously distributed at high CW levels.

III.B.2. Copper Alloy Void Formation Due to Electron Irradiation

Addition of solute to copper has been found to either reduce or enhance void formation during HVEM irradiation, depending on the nature and concentration of the solute.^(10,55,75,114,119,120,126) (See Table 3 for details.) Makin⁽¹¹⁴⁾ found that Cu-1% Ag and Cu-1% Cd (pre-injected with Ar) exhibited a shorter incubation period and larger swelling relative to pure Cu when examined after irradiation to 12 dpa ($K = 0.8$) at 250°C. Barlow⁽¹¹⁹⁾ found that Cu-0.1 wt.% Ag behaved similar to pure copper at all irradiation temperatures, while Cu-1 wt.% Ag had a higher swelling rate than pure Cu at 150-250°C due to an increased void number density. At 350-450°C, the alloy swelling rate was the same as for pure Cu. Takeyama et al.⁽¹⁰⁾ observed that the Ag solute was depleted in the matrix immediately surrounding the voids, with an enriched region at intermediate distances from the voids.

The addition of Be, Fe or Ni solute to copper apparently suppresses void swelling during HVEM irradiation. Makin⁽¹¹⁴⁾ did not observe any void formation in Cu-1% Be irradiated to 100 dpa ($K = 0.8$) at 250°C. No reason was given for this void-suppressing ability of the Be solute. Takeyama et al.^(10,55) have found that the void swelling, number density and growth rate of Cu-2 at% Fe were smaller than the corresponding values for Cu-2 at% Ag and pure copper for HVEM irradiation temperatures of 150-300°C. The Cu-Fe alloys exhibited a longer transition period prior to reaching a steady-state swelling

rate as compared to pure copper. After this transition period (3-6 dpa), the void swelling rate for Cu-Fe was observed to be comparable to that of pure copper.⁽⁵⁵⁾ Solute enrichment was observed in the matrix surrounding the voids.⁽¹⁰⁾ Void swelling was suppressed the most in as-quenched Cu-Fe specimens. Aged Cu-Fe exhibited intermediate suppression of void formation; swelling increased with increasing aging time. Voids were observed to preferentially nucleate near coherent precipitates. In general, void swelling increased as the amount of Fe in solution decreased.⁽⁵⁵⁾ It was suggested that the suppressed void formation in Cu-Fe was due to enhanced solute segregation effects, which inhibit the flow of vacancies to voids.⁽¹⁰⁾ Takeyama⁽⁷⁵⁾ has observed void formation in copper alloyed with 2 at% of either Ag, Fe, Ni, or Si following HVEM irradiation to 10 dpa at 100-300°C. No quantitative results were given for the Cu-Ni and Cu-Si alloys, but it appears that Cu-Ag swelled the most (6%), followed by Cu-Fe, Cu-Ni and Cu-Si.

Barlow⁽¹¹⁹⁾ and co-workers^(120,126) have extensively studied loop and void formation in Cu-Ni alloys (1, 2, 5, 10 wt.% Ni) as a function of temperature and HVEM dose. They found that Cu-Ni alloys are very resistant to void swelling, with no observation of voids for solute concentrations greater than 10% Ni even after HVEM irradiation doses of ~ 100 dpa. Plots of swelling vs. Ni content for different temperatures showed that swelling either decreased immediately, or else increased initially and then decreased with Ni concentration. In general, as temperature increased a greater Ni concentration was required to suppress void swelling. They determined that the swelling resistance was due to suppressed void growth as opposed to suppressed void nucleation. The mean void diameter was observed to decrease dramatically as the solute concentration was increased from 1% to 2% Ni. They attributed this

suppression of growth to the formation of submicroscopic radiation-induced nickel clusters which act as interstitial traps, thereby increasing point defect recombination.⁽¹²⁶⁾

III.B.3. Pure Copper Loop Formation Due to Electron Irradiation

Interstitial loops have been found in electron-irradiated copper for irradiation temperatures below 400°C. The details of some of these investigations are given in Table 3.

Makin⁽¹²⁷⁾ was the first to observe displacement damage in pure copper, which occurred during a room temperature HVEM irradiation. Black spot clusters nucleated during the first few minutes of irradiation and grew to become mainly perfect interstitial loops. Ipohorski and Spring⁽¹²⁸⁾ and then Fisher⁽¹¹⁶⁾ expanded upon Makin's work by examining in detail the various factors influencing loop formation. It was found that loop density decreased and size increased with increasing irradiation temperature, until at 400°C only a few large ($\geq 1 \mu\text{m}$) loops formed. Denuded zones at surfaces (60 nm deep at $\sim 20^\circ\text{C}$) and at grain boundaries increased in width with temperature. The loop size has been found to increase directly with irradiation time until the loops begin to overlap.⁽¹²²⁾ Recent studies have shown that the loop density decreases slowly with increasing HVEM irradiation temperature up to about 300°C; the loop density then falls off very rapidly.^(122,129,130) Stathopoulos⁽¹³⁰⁾ measured the width of the loop-denuded zones at the foil surfaces as a function of temperature, and found that it increased to $\sim 30 \text{ nm}$ at 320°C. This denuded zone width is much smaller than previously reported widths mentioned above (cf. Refs. 116, 128). Dislocation loop parameters were measured for irradiation temperatures from 140-320°C and were found to be in good agreement with theoretical predictions.

Barlow⁽¹¹⁹⁾ observed continuous nucleation of two types of interstitial loops during irradiation: Frank faulted loops lying on $\{111\}$ planes ($b = a/3$ $[111]$), and glissile prismatic loops on variable habit planes with $b = a/2$ $[110]$. The apparent activation energy for this loop growth was measured at 0.35 eV.⁽¹²⁶⁾ At intermediate temperatures, some authors have reported that vacancy clusters occur in addition to interstitial loops. Yoshida and Kiritani⁽¹³¹⁾ found that a room temperature HVEM irradiation of copper resulted in the inhomogeneous nucleation of vacancy clusters along with the usual interstitial loops. Upon extended irradiation, these clusters began to order and formed arrays in the $\langle 100 \rangle$ direction. The clusters were assumed to be stacking fault tetrahedra (SFT) or else voids and were preferentially found in thinner regions of the foil. A recent study has confirmed that these ordered arrays of clusters are SFT.⁽¹³²⁾

Kiritani et al.⁽¹³³⁾ studied the effect of an elevated temperature (720 K) HVEM irradiation on the subsequent observable radiation damage at intermediate temperatures (320 K). They found that the high-temperature pre-irradiation, which produced no observable radiation damage, caused virtually complete suppression of interstitial cluster formation normally found during a 320 K irradiation. They deduced that submicroscopic vacancy clusters formed during the high temperature pre-irradiation, and these clusters acted as interstitial sinks during the subsequent irradiation, thereby inhibiting interstitial clustering. Shimomura et al.⁽¹²⁹⁾ found that the interstitial loop density of copper containing quenched-in hydrogen was a factor of ten larger than the loop density of annealed copper for irradiation temperatures between 20-150°C.

There have been several investigations of the behavior of copper during annealing after a low-temperature HVEM irradiation.^(121,134-137) Jäger et al.⁽¹³⁴⁾ found that visible defect clusters form at an irradiation temperature of 10 K for doses of 5-10 dpa. Interstitial clusters become visible on {111} planes for lower dose irradiations (≤ 1 dpa) only after annealing to 50-120 K. No additional clusters formed during annealing above 120 K until a temperature of 470 K was reached (vacancy clusters). Ohr⁽¹³⁵⁾ had previously found similar results, except that he observed vacancy cluster formation after annealing above 360 K. Ohr determined that 40% of the loops were vacancy-type at an annealing temperature of 525 K. Ehrhardt and Schlagheck⁽¹³⁶⁾ and Haubold and Martinsen⁽¹³⁷⁾ determined from x-ray scattering measurements on copper irradiated with 3 MeV electrons at 5 K that vacancy clusters began forming upon annealing above 200 K. Interstitials began to cluster on both {111} and {110} planes at temperatures above 40 K.⁽¹³⁶⁾

III.B.4. Copper Alloy Loop Formation Due to Electron Irradiation

There have been relatively few systematic studies on the effect of alloying on dislocation loop nucleation and growth in copper during electron irradiation. Barlow⁽¹¹⁹⁾ and Leffers et al.⁽¹²⁰⁾ have studied interstitial loop growth parameters in Cu-Ni alloys as a function of temperature and dose following HVEM irradiation. Kosel and Washburn⁽¹³⁸⁾ noted that loop growth was induced at lower damage rates in Cu-Al alloys containing smaller solute concentrations, i.e., loop growth was easier for alloys having higher stacking energies. The climb rate of these prismatic interstitial loops appeared to be controlled by the rate of jog nucleation. Kinoshita and Mitchell^(43,139) observed vacancy loop formation in Cu-Be during HVEM irradiation. Frank-type interstitial loops were created on {111} planes in thin regions of the foil

where Cu-Be precipitates were not present. This observation was attributed to segregation of Be atoms to the surface during irradiation, which caused a copper-rich region. These loops were not observed in regions thicker than about 0.1 μm and their kinetic behavior corresponded to the case in pure metals where surfaces are the dominant sinks for interstitial atoms. Mukai and Mitchell⁽¹⁴⁰⁾ have recently studied the nature of dislocation loops in the ordered alloys Cu_3Au and CuAuI following HVEM irradiation at 300°C. Loop habit planes were identified.

TABLE 3. Void and Selected Dislocation Loop Studies in Electron-Irradiated Copper and Copper-Base Alloys

Specimen Purity/ Alloy Concent.	Electron Energy (MeV)	Flux ($10^{23}/m^2-s$)	Fluence ($10^{25}/m^2$)	Dose (dpa, $K=0.8$)	Irradiation Temp. ($^{\circ}C$)	Defect*	Mean Diameter (nm)	Density ($10^{20}/m^3$)	Swelling $\Delta V/V$ (%)	Comments	Ref.
99.999%	1	11	-	65	250	V	-	5	10	160 nm denuded zone at surfaces.	114
99.999% + Ar preinj.	1	(0.006 dpa/s)	-	95	250	V	-	10	17	Enhanced void nucleation due to Ar preinjection.	
99.995%	1	-	-	7	250	L,V	8	1.6	0.004	Effect of cold working: Higher initial dislocation density increases void density. (115,117) Maximum swelling at $\sim 50\%$ CW ($\rho_d = 1 \times 10^{15}/m^2$). (115) Data at other CW levels also given in Ref. 115. Swelling determined from swelling rate assuming given dose levels (8-15 dpa); however, doses as high as 60 dpa may have been investigated, (115) with resultant higher swelling levels.	117
99.999% annealed	1	20	-	15 ⁺ 12 ⁺ 10 ⁺ 8 ⁺	250 300 350 450	V V V V	~ 25 ~ 30 ~ 50 ~ 125	~ 5 ~ 3 ~ 1.5 ~ 0.3	~ 0.3 ~ 0.6 ~ 1.2 ~ 4		115, 123
50% CW	1	20	-	15 ⁺ 12 ⁺ 10 ⁺ 8 ⁺	250 300 350 450	V V V V	~ 25 ~ 25 ~ 30 ~ 90	~ 20 ~ 12 ~ 10 ~ 1.5	~ 1.3 ~ 1.5 ~ 2 ~ 5		
90% CW	1	20	-	15 ⁺ 12 ⁺ 10 ⁺ 8 ⁺	250 300 350 450	V V V V	~ 20 ~ 25 ~ 30 ~ 80	~ 10 ~ 4 ~ 5 ~ 1	~ 0.5 ~ 0.7 ~ 1.6 ~ 1.6		

TABLE 3. Void and Selected Dislocation Loop Studies in Electron-Irradiated Copper and Copper-Base Alloys
(Continued)

Specimen Purity/ Alloy Concent.	Electron Energy (MeV)	Flux ($10^{23}/m^2-s$)	Fluence ($10^{25}/m^2$)	Dose (dpa, $K=0.8$)	Irradiation Temp. ($^{\circ}C$)	Defect*	Mean Diameter (nm)	Density ($10^{20}/m^3$)	Swelling $\Delta V/V$ (%)	Comments	Ref.
99.995% deformed	1	~ 2	-	6	250	L, V	6	1.6	0.002	Void formation above 300°C	118
99.99% pre-irrad. to 1 dpa at 100°C	1	(1.3×10^{-3}) dpa/s		35	400	L, V	-	4	2.2	occurred only if pre-irradiation dislocation structure present.	
				35	450	L, V	-	1.4	4.7		
				35	500	L, V	-	0.8	5.8		
				35	550	L, V	-	0	0		
99.99% degassed	1	1.3×10^{-3} dpa/s	-	14	250	L, V	-	0.4	0.64	Dislocation density decreases from $3 \times 10^{13}/m^2$ to $8 \times 10^{12}/m^2$ with temperature.	118
				14	300	L, V	~ 80	0.6	1.7		
				14	344	L, V	~ 120	0.25	2.8		
				14	400	L, V	-	0.03	1.8		
				14	450	L, V	-	0	0		
99.999%	1	23 (0.015 dpa/s)	-	30	150	L, V	20	10	-	Swelling linear with fluence following an incubation period $\sim 2-10$ dpa.	119, 120
				90	250	L, V	30	4	1.0	Swelling rate is temp.-dependent with a maximum value of $\sim 0.5\%/dpa$. Void shrinkage at 550°C.	
				30	350	L, V	65	3	4.0		
				30	400	L, V	110	1	10		
				30	450	L, V	190	0.6	13.7		
				30	500	L, V	285	0.02	2.5		
				30	550	-	0	0	0		
99.999%	0.65	3	330	10	250	V	-	0.7	~ 8.2	Swelling rate $\sim 0.9\%/dpa$.	55
"pure"	1	-	-	12	220	L, V	~ 180	~ 5	~ 1.5 ?		122

TABLE 3. Void and Selected Dislocation Loop Studies in Electron-Irradiated Copper and Copper-Base Alloys
(Continued)

Specimen Purity/ Alloy Concent.	Electron Energy (MeV)	Flux ($10^{23}/\text{m}^2\text{-s}$)	Fluence ($10^{25}/\text{m}^2$)	Dose (dpa, $K=0.8$)	Irradiation Temp. ($^{\circ}\text{C}$)	Defect*	Mean Diameter (nm)	Density ($10^{20}/\text{m}^3$)	Swelling $\Delta V/V$ (%)	Comments	Ref.
99.999%	1	-	-	32 45	300 450	V V	- -	7 0.75	- -	No voids when foil thickness < 500 nm. Vacuum environ- ment has no effect.	124
99.999% > 30 appm He no He > 100 appm He	1 1 1 1 1	23 (0.015 dpa/s)	-	20	250 250 450 450	V V V V	- - - -	4.5 17 0.6 2.2	- - - -	Helium increases void density at all temperatures.	119
1% Ag	1	11	-	12	250	V	-	-	13	Addition of Ag either in- creases (114,119) or slightly decreases (75) void swelling compared to pure copper.	114 119
0.1 wt% Ag	1	23 (0.15 dpa/s)	-	30	150 250 350 400	V V V V	16 35 70 100	9 6.5 2.5 2.2	- - - -		
1 wt% Ag	1	23	-	30	150 250 350 400	V V V V	~ 15 30 70 95	> 20 13.5 3 2	- - - -		
2 at % Ag	0.65	3	-	10	250	V	-	2	6		75
0.1, 1% Cd	1	11	-	12	250	V	-	-	-	Cd enhances swelling com- pared to copper.	114

TABLE 3. Void and Selected Dislocation Loop Studies in Electron-Irradiated Copper and Copper-Base Alloys
(Continued)

Specimen Purity/ Alloy Concent.	Electron Energy (MeV)	Flux ($10^{23}/m^2-s$)	Fluence ($10^{25}/m^2$)	Dose (dpa, $K=0.8$)	Irradiation Temp. ($^{\circ}C$)	Defect*	Mean Diameter (nm)	Density ($10^{20}/m^3$)	Swelling $\Delta V/V$ (%)	Comments	Ref.
1.2 at % Be	1	11	-	100	250	-	-	-	0	Be completely suppresses void swelling.	114
2 at % Fe (quenched)	0.65	3	-	8	250	V	-	0.5	1.8	Fe in solution suppresses void swelling by increasing void incubation dose.	55
aged 1 hr	0.65	3	-	8	250	V	-	1.5	3.5	Eventual swelling rate similar to pure Cu.	
aged 290 hr	0.65	3	-	8	250	V	-	0.4	5		
1 wt % Ni	1	23 (0.15 dpa/s)	-	90 45 30 30 30 90 45 30 30 30 90 45 30 30 30 23	250 350 450 500 550 250 350 450 500 550 250 350 450 500 550 250 350 450 500 550 250 300-500 550	L, V	30 80 180 310 - 16 20 105 220 150 10 12 55 180 345 10 0 120	3.5 1.2 0.18 0.04 - 9 3.3 0.36 0.31 0.025 9.5 3.5 0.46 0.16 0.025 8 0 0.03	0.6 2.4 4.0 5.9 0 0.1 0.13 1.5 9.1 0.3 < 0.1 < 0.1 0.3 4.5 3.5 < 0.1 0 0.3	Addition of Ni generally reduces void swelling and shifts peak swelling temperature upwards. Void swelling increased compared to copper under certain conditions. Reduced swelling due to lower void growth rate.	119, 120
2 wt % Ni	1	23	-	90 45 30 30 30 90 45 30 30 30 90 45 30 30 30 23	250 350 450 500 550 250 350 450 500 550 250 350 450 500 550 250 300-500 550						
5 wt % Ni	1	23	-	90 45 30 30 30 90 45 30 30 30 90 45 30 30 30 23	250 350 450 500 550 250 350 450 500 550 250 350 450 500 550 250 300-500 550						
10 wt % Ni	1	23	-	90 45 30 30 30 90 45 30 30 30 90 45 30 30 30 23	250 350 450 500 550 250 350 450 500 550 250 350 450 500 550 250 300-500 550	- V					

TABLE 3. Void and Selected Dislocation Loop Studies in Electron-Irradiated Copper and Copper-Base Alloys
(Continued)

Specimen Purity/ Alloy Concent.	Electron Energy (MeV)	Flux ($10^{23}/\text{m}^2\text{-s}$)	Fluence ($10^{25}/\text{m}^2$)	Dose (dpa, $K=0.8$)	Irradiation Temp. ($^{\circ}\text{C}$)	Defect*	Mean Diameter (nm)	Density ($10^{20}/\text{m}^3$)	Swelling $\Delta V/V$ (%)	Comments	Ref.
2 at % Ni	0.65	3	-	7	300	V	-	-	?	Segregation of Ni onto voids; void nucleation near dislocations.	11, 75
2 at % Si	0.65	3	-	10	150	-	-	-	0		75
high purity	0.58	0.3	10	-	~ 20	L	20	-	-	Interstitial loops grow initially. Later, vacancy clusters also form.	127
h.p.; quenched or deformed	0.58	0.3	7	-	~ 20	L	-	V. High	-	Very rapid loop growth, coalescing into dense dis- location tangles.	127
99.998%	0.6	1.2	-	-	~ 20	L	< 1000	-	-	60 nm denuded zone near surface; no defects in foil > 100 nm thick. Loops on (111) planes.	128
"pure"	1	-	-	3.8 1.5 1.2 0.6	140 220 250 320	L L L L	220 270 300 500	1.8 1 0.7 0.16	- - - -	Interstitial loop growth linear with fluence until loop interaction occurs (0.6-3.8 dpa).	122

TABLE 3. Void and Selected Dislocation Loop Studies in Electron-Irradiated Copper and Copper-Base Alloys
(Continued)

Specimen Purity/ Alloy Concent.	Electron Energy (MeV)	Flux ($10^{23}/\text{m}^2\text{-s}$)	Fluence ($10^{25}/\text{m}^2$)	Dose (dpa, $K=0.8$)	Irradiation Temp. ($^{\circ}\text{C}$)	Defect*	Mean Diameter (nm)	Density ($10^{20}/\text{m}^3$)	Swelling $\Delta V/V$ (%)	Comments	Ref.
99.999%	1	9	-	?	20	L	-	5.5	-	Interstitial loop density decreases rapidly above 300°C. Loop growth rate $\sim 1/T$.	130
					100	L	-	4.2	-		
					150	L	-	3.1	-		
					250	L	-	2	-		
					325	L	-	0.15	-		
99.9999% Cu + H ₂	1.25	6	-	?	100	L	-	4	-	Interstitial loop density much higher in copper con- taining quenched-in hydrogen.	129
		6	-	?	100	L	-	40	-		
1-5 wt % Ni 10 wt % Ni	1	20	-	-	250-500	L	-	-	-	Interstitial loop growth is slower for Cu-10% Ni, but similar for all the other Cu-Ni alloys and pure Cu.	126
		20	-	-	250-500	L	-	-	-		

* V = void, L = (interstitial) loop

III.C. Ion Irradiations

There have been several investigations of void and loop formation in ion-irradiated copper and copper alloys. The results of these studies are summarized in Table 4.

III.C.1. Pure Copper Void Formation Due to Ion Irradiation

Mazey and Menzinger⁽¹⁴¹⁾ observed void formation of copper which had been pre-implanted with helium and then irradiated with either C, Cu or Ni ions to doses greater than 10 dpa ($K = 0.3$) at temperatures from 350-450°C. No quantitative information was given regarding the extent of void formation. Leister⁽¹⁴²⁾ observed void swelling in copper following 200-keV Cu ion irradiation at temperatures 400-575°C. Irradiation to a dose of 30 dpa ($K = 0.4$) resulted in peak void swelling of about 2%.

A comprehensive investigation of the effect of ion bombardment on void swelling was carried out by several French scientists in the early 1970's. The initial results of this work were presented by Adda,⁽⁸⁷⁾ and the completed work was reported in detail by Glowinski et al.⁽¹⁴³⁻¹⁴⁶⁾ The influence of various irradiations and materials parameters on the nucleation and growth of voids and dislocation loops was examined for high-purity copper irradiated with 500-keV Cu ions. Specifically, the influence of irradiation temperature, dose rate, dose, foil thickness (effect of free surfaces), dislocation structure, and gas content was studied.

Void swelling occurred in high purity non-degassed copper irradiated at a dose rate of 1×10^{-4} dpa/sec ($K = 0.4$) for temperatures from 400-500°C.⁽¹⁴⁴⁾ Void size increased from 30 to 90 nm as the temperature went from 400 to 450°C, while the void density remained the same. The maximum void swelling of

non-degassed copper occurred at 500°C and a dose rate of 1×10^{-3} dpa/sec ($K = 0.4$) with a value of 9% for a damage level of 15 dpa ($K = 0.4$).

Increasing the ion damage rate from 1×10^{-4} dpa/sec to 1×10^{-3} dpa/sec caused the swelling curve to shift upward in temperature by 50°C.⁽¹⁴⁴⁾ The swelling peak of the high dose-rate case consisted of a lower density of larger voids as compared to the low dose-rate case. Compared with neutron irradiations⁽⁹⁰⁾ that occurred at a dose rate of 8×10^{-8} dpa/sec ($K = 0.3$), the peak swelling temperature for copper ion-bombarded at a damage rate of 1×10^{-4} dpa/sec ($K = 0.4$) was increased by 115°C.

For a constant temperature and dose rate, the void density remained constant and the void size increased with damage level.⁽¹⁴⁵⁾ Below a fluence of 1.5 dpa ($K = 0.4$), swelling as a function of fluence increased at more than a linear rate; for fluences greater than 1.5 dpa the swelling rate was less than linear. No voids were observed if foils of thickness $\lesssim 200$ nm were irradiated.⁽¹⁴⁴⁾ The absence of defect clusters in the very thin foils had two possible causes: (1) depression of point defect concentrations due to loss to the surface, or (2) loss of dislocations to the surface. This would decrease the dislocation density in these regions below the level required for void formation.

Several general conclusions were reached regarding the experimental evidence for the role of dislocations in void formation. First, voids almost always nucleated near interstitial loops or dislocation lines, on the compression side of the dislocation.⁽¹⁴³⁻¹⁴⁵⁾ Secondly, some minimum dislocation density was necessary for void formation, and there was a direct correlation between void number density and dislocation density.⁽¹⁴⁵⁾ Finally, void growth was affected by the vicinity of a dislocation -- void size increased

very rapidly during the early stages of void growth (at fluences $\lesssim 1.5$ dpa, $K = 0.3$) when all voids were in the close proximity of dislocations. All the observations are evidence that dislocations act as biased sinks absorbing interstitials preferentially to vacancies, thereby creating an excess of vacancies that precipitate into voids.

A comprehensive investigation of the effect of gas on void nucleation was also undertaken by Glowinski et al.⁽¹⁴⁴⁻¹⁴⁶⁾ High-purity copper which had not been outgassed readily formed voids at doses of 1.5 dpa ($K = 0.4$). On the other hand, copper which had been partially outgassed exhibited a bimodal size distribution (mean void diameters of 75 nm and 130 nm) along with a reduction in the amount of swelling. Copper specimens which has been completely outgassed did not show any void formation even when irradiated at 450° to damage levels of 15 dpa ($K = 0.4$) -- only black spots and some vacancy loops were visible. The absence of voids was attributed to the removal of residual gas during the high-vacuum anneal.⁽¹⁴³⁻¹⁴⁶⁾ The initial gas content of specimens used in Ref. 143 was not specified, but those in Refs. 144-146 contained less than 48 ppm O, 12.4 ppm H, 14 ppm N, and 48 ppm C.

Pre-implantation of outgassed copper specimens with helium or oxygen resulted in void formation during irradiation,⁽¹⁴⁴⁻¹⁴⁶⁾ thereby giving strength to the argument that gas is necessary for void nucleation. The presence of helium in outgassed specimens was found to enhance void swelling relative to pure (non-degassed) copper; the magnitude of swelling increased, the swelling temperature range was widened, and the peak swelling temperature was shifted upwards. The behavior of swelling with respect to gas content was different for the oxygen and helium injected specimens. For concentrations less than 30 ppm, helium was somewhat more efficient than oxygen in nucleating both voids

and interstitial loops. At higher gas concentrations, the void density decreased for helium but remained constant for oxygen. This was explained in terms of the different solubilities of the two gases in copper. It was concluded that gas enhanced void formation by acting to stabilize the vacancy clusters. A subsequent investigation of the annealing characteristics of the voids present in the helium and oxygen-injected specimens showed that oxygen has a very large effect on the surface energy of the voids, while helium has a negligible effect.⁽¹⁴⁷⁾ An oxygen concentration of 100 ppm reduced the surface energy by a factor of 1.7.

Several degassed copper specimens that were implanted with carbon prior to irradiation contained neither voids nor dislocation networks.⁽¹⁴⁶⁾ Specimens implanted with oxygen or helium in conjunction with carbon exhibited less swelling than if the carbon was absent. This indicated that carbon inhibits void formation by acting as a point defect trap.

Swelling did not occur in specimens that had been implanted with hydrogen prior to irradiation.⁽¹⁴⁶⁾ Three types of samples were implanted with hydrogen: non-degassed, degassed, and degassed copper which was subsequently work-hardened. None of the specimens contained voids or dislocation networks. Either the hydrogen diffused out of the specimens, or it had no effect on damage formation. The absence of voids in the non-degassed copper was not explained.

One criticism which may be raised concerning the Glowinski gas effects work is the questionable quantitative results attainable with bombarding ion energies of 500 keV. All of the TEM analysis was performed in the peak damage region, where injected interstitial effects may be significant.⁽¹⁴⁸⁾ At this energy the peak damage region is located at a depth of 150 nm.⁽¹⁴⁴⁾ Therefore

the observed results concerning void formation may be greatly influenced by the free surface, as was previously mentioned. Buckley et al.⁽¹²⁴⁾ found that void swelling fell to zero during HVEM irradiation of copper at 250-300°C for foil thicknesses of less than 500 nm. Further support for this argument may be found from the fact that Glowinski et al. did not observe void formation in (non-outgassed) high-purity copper which has been pre-injected with hydrogen,⁽¹⁴⁶⁾ contrary to expectations.

Knoll⁽⁷⁾ irradiated outgassed and non-outgassed high-purity copper with 14-MeV neutrons (peak damage region depth $\gtrsim 2 \mu\text{m}$) in an attempt to determine the effect of outgassing on void formation. Unfortunately, no voids were observed in either case following irradiation at 400-500°C to a peak damage level of 3-10 dpa ($K = 0.3$). The absence of voids was attributed to the high purity of the copper (lack of gaseous impurities), in support of the Glowinski et al. results. A recent void nucleation calculation⁽¹⁴⁸⁾ indicates that the swelling regime for ion-irradiated pure copper in the absence of gas should be from 100-250°C. Therefore, it appears that the presence of gas may simply shift the upper range for void formation to higher temperatures; Knoll⁽⁷⁾ may have been at too high of an irradiation temperature to observe void formation in copper that did not contain any gas. It appears that more basic work regarding the effect of gas on void nucleation is needed.

III.C.2. Copper Alloy Void Formation Due to Ion Irradiation

There are very few known studies of void formation in ion-irradiated copper alloys (see Table 4). Mazey and Menzinger⁽¹⁴¹⁾ found that Cu-Ni alloys were very resistant to void formation, in agreement with previous neutron⁽⁹⁰⁾ and later HVEM^(119,120,126) studies. No voids were observed in alloys containing greater than 2% Ni solute for irradiation doses well in excess of 30

dpa. They proposed that fine-scale clusters of Ni atoms were acting as point defect traps, thereby inhibiting vacancy agglomeration into voids. This hypothesis was later reaffirmed in an HVEM study^(120,126)

Venker et al.⁽¹⁵⁰⁾ investigated the influence of fast diffusing substitutional solutes on the swelling behavior of ion-irradiated Cu alloys. Alloys of Cu-0.7% Mg and Cu-0.7% In were found to cause reduced swelling compared to pure Cu when irradiated with 150 keV Cu ions. The maximum swelling temperature was shifted towards lower temperatures by 20-30°C for the alloys as compared to pure Cu. The reduction in swelling was attributed to the idea that some of the fast diffusing solute atoms occupy interstitial positions and consequently there is an increased probability for vacancy-interstitial annihilation to occur in these alloys. The shift in the peak swelling temperature was explained by an elevation of the mean diffusion coefficient for the two Cu alloys.

Knoll^(7,36) has irradiated Cu-3.4 at% Be, Cu-1%Co and Cu-1%Fe specimens with 14-MeV Cu ions to peak damage levels of 1.5-15 dpa ($K = 0.3$) at temperatures 350-525°C. No void formation was observed in the Cu-Be and Cu-Co alloys for any of the irradiation conditions.⁽⁷⁾ Voids were observed in a quenched Cu-Fe specimen which was irradiated at 400°C to 1 dpa ($K = 0.3$). The lack of void formation in the copper alloys was proposed to be due to lack of nucleating agents (gaseous impurities), and also due to point defect trapping at the interface of coherent precipitates. For the Cu-Be alloy, it was also speculated that the absence of voids may be due to Be solute interacting with the point defects and/or Cu-Be precipitates acting as point defect sinks.⁽⁷⁾

Leister⁽¹⁴²⁾ has recently reported the results of a thorough investigation of void formation in copper alloys. Alloys containing 0.1 at.% and 1%

of Pt, Ni, Au, Be, Ag, and Sb were irradiated with 200 keV Cu ions to a damage level of 30 dpa ($K = 0.4$) at temperatures between 400 and 600°C. All of the 0.1% alloys exhibited enhanced swelling as compared to pure copper, with fast diffusing solutes (Au, Ag, Be, Sb) causing slightly more swelling than slow diffusing solutes. No correlation was observed between swelling and the copper-solute misfit size or alloy electronegativity. The 1% alloys all showed reduced swelling as compared to pure copper. The Cu-1% Au and Cu-1% Be alloys did not exhibit void formation at any temperature. No explanation for the observed results was proposed. An additional investigation of the effect of Ni solute concentration on void swelling was carried out. Swelling was reduced with increasing Ni content, and no swelling was observed for Ni solute concentrations greater than 10%. Increasing Ni content from 0.1% to 1% caused a delay in the incubation dose and a lower steady-state void density. Swelling in Cu-0.1% Ni began to saturate at a dose of 60 dpa ($K = 0.4$) with a value of 10-12%. The Cu-1% Ni alloy exhibited swelling saturation at a dose of 40 dpa ($K = 0.4$) with a value of 3-4%. It is probably not appropriate to attempt to extract any quantitative information out of the Leister study due to the low energy of the ions used to create the displacement damage -- surface effects⁽¹²⁴⁾ and injected interstitial ion effects⁽¹⁴⁸⁾ will certainly exert a large influence on the void nucleation and growth. However, the observed qualitative trends may still be applicable.

A recent investigation of the effect of 14-MeV Cu ion irradiation on the microstructure of cold-worked plus aged Cu-0.12 at.% Zr and Cu-0.8% Cr-0.12% Zr-0.4% Mg revealed that no voids were observed following irradiation to peak damage levels of 15 dpa ($K = 0.3$) at temperatures of 400-550°C.^(148,149) However, a low density of large voids was observed in an annealed Cu-Zr sample

following irradiation to 15 dpa at 300°C. This indicates that the swelling regime for these alloys in the absence of gaseous nucleating agents may be restricted to temperatures less than 300°C ($0.4 T_m$).

III.C.3. Pure Copper Loop Formation Due to Ion Irradiation

Loop formation in copper following ion irradiation has been studied by several investigators.^(103,151-170) Ruhle⁽⁸²⁾ has summarized most of the early ion-irradiation loop formation studies in copper. Heavy ion irradiation-induced loop formation in pure copper has also been recently reviewed by Stathopoulos.⁽¹⁵¹⁾ A summary of some of the loop formation studies in copper and copper alloys following ion irradiation is presented in Table 4. The general trends may be summarized as follows.

Irradiation of copper with low-energy (30-150 keV) Cu ions at ambient temperatures has been found to produce predominantly vacancy-type loops 1.0-9.0 nm in diameter with Burgers vector $b = a/3 \langle 111 \rangle$.^(157,158,160,162,165,167) The loops were often faulted or dissociated, and were superimposed on a background of irresolvable "blackspot" clusters. The vacancy loops are formed by collapse of the vacancy-rich core of the displacement cascade on close-packed planes.⁽¹⁶²⁾ Few interstitial loops are formed during low-energy heavy ion bombardment due to a high loss rate of interstitials to the nearby free surface. For irradiation temperatures above ambient conditions, an increasing percentage of the vacancy loops are found to be unfaulted with $b = a/2 \langle 110 \rangle$ and stacking fault tetrahedra are also observed.⁽¹⁶²⁾ The loop density and size was found to decrease dramatically for 30 keV Cu^+ ion irradiation at temperatures above 300°C. Stathopoulos et al.⁽¹⁶⁷⁾ have recently observed that the effect of a 30 keV Cu^+ ion irradiation at ambient temperatures is to cause exclusive formation of vacancy-type Frank loops ($b = a/3 \langle 111 \rangle$) which

were equally distributed on the four {111} planes. Their reported size distributions appear to be well described by a log-normal curve. Knoll⁽⁷⁾ reported the formation of scattered dislocation loops approximately 30 nm in diameter along with dislocation tangles following a 14-MeV Cu ion irradiation to a peak damage level of 4 dpa ($K = 0.3$) at 400°C.

There have been at least two investigations of the effect of ion irradiation temperature on loop formation over the temperature range of 90-300 K.^(165,168) Schindler et al.⁽¹⁶⁵⁾ found that the cluster size following irradiation with 30 keV Cu ions showed a step-like increase at an irradiation temperature of about 200 K. Laupheimer et al.⁽¹⁶⁸⁾ repeated the above study and did not observe this step-like increase -- the loop diameter was found to be constant ($d = 3.6$ nm) over the irradiation temperature range 6-295 K.

Bombardment of copper with gas ions results in a different microstructure as compared to heavy ion irradiation.^(152,163) The gas atoms act as impurities in the target, which lead to interstitial loop formation often accompanied by small vacancy clusters. Bombardment of copper with 20-60 keV H^+ and 38 MeV He^{++} was found to produce large interstitial loops and 2 nm diameter vacancy clusters.

III.C.4. Copper Alloy Loop Formation Due to Ion Irradiation

Copper alloy loop studies have centered on the effect of stacking fault energy on loop formation during ion bombardment. In Cu-10% Al and Cu-16% Al, the lower stacking fault energy caused dislocation loops to dissociate more easily into S.F. tetrahedra.^(103,164) However, the basic damage structure remained similar to that of pure copper.

Researchers at Harwell have recently extended these early results on loop formation in copper alloys, using 30-90 keV Cu or W ion irradiations conducted

at room temperature.^(169,170) Copper alloyed with Al, Ge, Si, Ni, Zn or Be (low stacking fault energy alloys compared to copper) were found to have a greater concentration of stacking fault tetrahedra due to loop dissociation. The alloys exhibited higher visible cluster concentrations as compared to pure copper, with the cluster concentration increasing with increasing solute content. No simple relationship was observed concerning the effect of alloying on the cluster size distribution. It was concluded that the same cluster formation mechanism operates in the alloys as in pure copper, i.e., athermal collapse of the vacancies in the displacement cascade to form small dislocation loops.

TABLE 4. Void and Selected Dislocation Loop Studies in Ion-Irradiated Copper and Copper-Base Alloys

Specimen Purity/ Alloy Concent.	Ion Energy (MeV)	Dose (dpa, K=0.4)	Dose Rate (10^{-4} dpa/s K=0.4)	Irradiation Temp. (°C)	Defect*	Mean Diameter (nm)	Density ($10^{20}/m^3$)	Swelling $\Delta V/V$ (%)	Comments	Ref.
high purity	0.5	2	1	300	-	-	-	0	Increasing dose rate by factor of 10 shifts peak swelling temperature upwards by 50°C. Foils contained residual gas. In thin regions of the foil (50-200 nm) only black spots form. Voids are visible in thicker regions or near dislocations.	87
				400	V	-	-	0.7		
				300	-	-	-	0		
				400	-	-	-	0		
				450	V	-	-	4		
h.p.	0.5	1.5	1.4	350	vL	-	-	0		144
				400	V	30	0.8	0.13		
				450	V	90	0.8	3.2		
				500	-	-	-	0		
				400	vL	-	-	0		
				450	V	100	0.6	3.4		
				500	V	210	0.2	9		
				530	V	220	0.06	3.2		
				550	V	-	0	0		
99.999%	0.2	30	500	400	-	-	< 0.1	0	Effect of temperature on void swelling. Hydrogen may have been introduced during pre-irradiation electropolish (D2 electrolyte).	142
				425	V	-	1.5	0.4		
				450	V	-	2.2	1.3		
				475	V	-	4.1	1.9		
				500	V	-	2.0	2.1		
				525	V	-	0.3	0.6		
				550	V	-	< 0.1	0.6		
				575	V	-	-	0		
				600	V	-	-	0		

TABLE 4. Void and Selected Dislocation Loop Studies in Ion-Irradiated Copper and Copper-Base Alloys
(Continued)

Specimen Purity/ Alloy Concent.	Ion Energy (MeV)	Dose (dpa, K=0.4)	Dose Rate (10^{-4} dpa/s K=0.4)	Irradiation Temp. (°C)	Defect*	Mean Diameter (nm)	Density ($10^{20}/m^3$)	Swelling $\Delta V/V$ (%)	Comments	Ref.
99.99%, thick foils	0.5	0.4	15	450	V	19	3.2	0.16	Effect of dose on void swelling. Loops, voids lie on or near dislo- cations. Line dislocation density is $0.8-7.0 \times 10^{13}/m^2$. Interstitial loops also noted. Foils contained residual gas. Linear swelling rate $\sim 0.2\%/dpa$ ($K=0.4$).	145
		0.85				27	3.4	0.43		
		1.5				34	4.0	0.88		
		5				42	3.2	1.41		
		15				66	1.8	3		
prethinned foil	0.5	15	15	450	V	100	0.6	3.4		
"pure"	0.15	80	-	500	V	-	-	0.6		150
h.p., as- rolled Kr ⁸⁵ doped	0.5	20	10	450	V	-	-	0.5	High sink density reduces swelling.	87
	0.5	20	10	450	-	-	-	0		
h.p., degassed at: 450°C 600°C 700°C	0.5	15	14	450	vL, iL, V	100	0.6	3.4	Degassing at high temperature in vacuum reduces or eliminates void formation at peak swelling temp. for nondegassed copper. Bimodal size distribution for partially degassed Cu. No voids, interstitial loops or network dislocations for 750°C degassing.	144
					V	75, 130	0.6	1		
					vL	-	-	~ 0		
h.p., degassed at 750°C, 6×10^{-10} torr	0.5	0.4	15	450	vL	-	-	0		145
		0.8			vL	-	-	0		

TABLE 4. Void and Selected Dislocation Loop Studies in Ion-Irradiated Copper and Copper-Base Alloys
(Continued)

Specimen Purity/ Alloy Concent.	Ion Energy (MeV)	Dose (dpa, K=0.4)	Dose Rate (10^{-4} dpa/s K=0.4)	Irradiation Temp. ($^{\circ}$ C)	Defect*	Mean Diameter (nm)	Density ($10^{20}/m^3$)	Swelling $\Delta V/V$ (%)	Comments	Ref.
MARZ grade	14	3.4(a)	17(a)	400	L	-	-	0	No void formation in high-purity copper in the absence of gas for $T_{irr} = 400-500^{\circ}$ C.	7
		11(a)	22(a)	450	L	-	-	0		
		3.4(a)	21(a)	500	-	-	-	0		
99.99%, He doped	0.5	15	15	450	V	75	0.8	4.1	1 x $10^{18}/m^2$ He preinject increases void density.	144
				530	V	190	0.2	12		
99.99%, degassed 1 ppm He 5 ppm He 15 ppm He 30 ppm He 100 ppm He	0.5	16	15	450	V	115	0.3	2.5	Preinjected helium increases void density at 450-500 $^{\circ}$ C. Dislocation density (ρ_d) equals $1.8-4 \times 10^{13}/m^2$ at 450 $^{\circ}$ C, $0.6-3 \times 10^{13}/m^2$ at 500 $^{\circ}$ C.	146
						105	0.6	4		
						93	0.9	4.5		
						90	1.0	5		
						95	0.4	1.5		
30 ppm He 50 ppm He 100 ppm He	0.5	16	15	500	-	-	0	0		
					V	210	0.1	5.7		
					V	150	0.6	14		
h.p. + 10 ppm He	46.5 0.1 0.1	10(a) > 100 > 100	-	400	V	-	-	-		141
				275-350	-	-	-	0		
				350-450	V	-	-	-		

TABLE 4. Void and Selected Dislocation Loop Studies in Ion-Irradiated Copper and Copper-Base Alloys
(Continued)

Specimen Purity/ Alloy Concent.	Ion Energy (MeV)	Dose (dpa, K=0.4)	Dose Rate (10^{-4} dpa/s K=0.4)	Irradiation Temp. (°C)	Defect*	Mean Diameter (nm)	Density ($10^{20}/m^3$)	Swelling $\Delta V/V$ (%)	Comments	Ref.
99.99%, degassed 7 ppm O 40 ppm O 105 ppm O 30 ppm O 70 ppm O 100 ppm O	0.5	16	15	450	V	135	0.3	4	Oxygen increases swelling and shifts to higher temperatures. $\rho_D = 1.7-5.3 \times 10^{13}/m^2$ at 450°C, $\rho_D = 3.5-5.5 \times 10^{13}/m^2$ at 500°C.	146
						130	0.3	3.7		
						120	0.27	2.5		
						-	0	0		
						245	0.074	6.3		
						220	0.15	10		
99.99%, 100 ppm H degassed, 100 ppm H deformed, 100 ppm H	0.5	16	15	450	-	-	-	0	No voids or network dislocations.	146
						-	-	0		
						-	-	0		
degassed, 30 ppm C	0.5	16	15	450	black spots, small VL			0	No voids or network dislocations. C inhibits vacancy cluster formation.	146
0.1 at % Ag 1 at % Ag	0.2	30	500	425	V	-	5.1	3.3	Suppressed swelling for increasing Ag conc. Data is from swelling peak (other temps. 400-600°C also investigated).	142
				525	V	-	1.1	0.5		

TABLE 4. Void and Selected Dislocation Loop Studies in Ion-Irradiated Copper and Copper-Base Alloys
(Continued)

Specimen Purity/ Alloy Concent.	Ion Energy (MeV)	Dose (dpa, K=0.4)	Dose Rate (10 ⁻⁴ dpa/s K=0.4)	Irradiation Temp. (°C)	Defect*	Mean Diameter (nm)	Density (10 ²⁰ /m ³)	Swelling $\Delta V/V$ (%)	Comments	Ref.
0.1 at % Au 1 at % Au	0.2	30	500	525 400-600	V -	- -	2 0	4.5 0	No voids observed in Cu-1 at % Au.	142
0.1 at % Be 1 at % Be	0.2	30	500	475 400-600	V -	- -	2.5 0	3.4 0	No voids in copper alloyed with > 1 at % Be.	142
3.4 at % Be	14	1.5-15(a)	10-20(a)	300-525	L	-	-	0	Dose, dose rate values are from the peak damage region.	7
1 at % Co	14	0.3-1.7(a)	12(a)	400,475	-	-	-	0	Dose rate at peak damage region.	7
1 at % Fe quenched aged	14	1-5(a) 1.1(a) 1.1(a) 1-5(a) 1.1(a)	4-20(a) ~ 4(a) ~ 4(a) 4-20(a) ~ 4(a)	500 450 400 400 350	- - V - -	- - 30 - -	- - 0.4 - -	0 0 0.06 0 0	Back-thinned or cross section speci- mens irradiated in both the quenched and aged condition at all temperatures.	7
0.7% In	0.15	80	-	480	V	-	-	0.13	Reduced swelling compared to copper for these fast-diffusing solutes.	150
0.7% Mg	0.15	80	-	480	V	-	-	0.2		
0.1 at % Ni	0.2	30 3 12 24 30	500	540 525 ?	V - V V V	- - - - -	10 - 0.4 2 2.3	4 0 1 2.5 3.2	No swelling in Cu-Ni for > 10% Ni concentration. Void formation inhibited in Cu-Ni by trapping at solute atoms or clusters. (141) Peak swelling enhanced in Cu-0.1% Ni,	142

TABLE 4. Void and Selected Dislocation Loop Studies in Ion-Irradiated Copper and Copper-Base Alloys
(Continued)

Specimen Purity/ Alloy Concent.	Ion Energy (MeV)	Dose (dpa, K=0.4)	Dose Rate (10^{-4} dpa/s K=0.4)	Irradiation Temp. ($^{\circ}$ C)	Defect*	Mean Diameter (nm)	Density ($10^{20}/m^3$)	Swelling $\Delta V/V$ (%)	Comments	Ref.
0.1 at % Ni	0.2	36	500	525 ?	V	-	2.5	6.9	reduced for larger alloy contents compared to pure copper. Void density saturates after ~ 30 dpa (K=0.4). Void swelling saturates after ~ 50 dpa (K=0.4). More complete information is given in Ref. 142 on temperature and dose dependence.	142
		42						9		
		48						9		
		60						10.7		
		30						0.6		
		30						0.7		
		12						0		
		24						1		
		36						2.7		
		48						3.3		
10 at % Ni	0.2	60	500	475 525 575	V	-	1.05	3.2	Other temps. investigated with 0.1 MeV ion irradiation to high doses. (141)	141
		30						0.4		
		30						< 0.1		
		30						0.5		
		11(a)						-		
								0		
0.1 at % Pt 1 at % Pt	0.2	30	500	475 500	V	-	1.5 0.32	3	Peak swelling enhanced for 0.1% alloys reduced for 1% alloys compared to pure copper. Temp. dependence 400-600°C was reported.	142
								0.7		
0.1 at % Sb 1 at % Sb	0.2	30	500	500 450	V	-	4 10	6		142
								1.5		

TABLE 4. Void and Selected Dislocation Loop Studies in Ion-Irradiated Copper and Copper-Base Alloys
(Continued)

Specimen Purity/ Alloy Concent.	Ion Energy (MeV)	Dose (dpa, K=0.4)	Dose Rate (10^{-4} dpa/s K=0.4)	Irradiation Temp. (°C)	Defect*	Mean Diameter (nm)	Density ($10^{20}/m^3$)	Swelling $\Delta V/V$ (%)	Comments	Ref.
0.15 at % Zr	14	15(a)	7-25(a)	400-550 100-250	-	- black spot damage	-	0 0	Cold-worked plus aged Cu-Zr has no observable void formation (cross- section analysis).	149, unpubl.
0.15 at % Zr, annealed	14	15(a)	7-25(a)	300	V	≥ 300	~ 0.001	~ 0		148
0.8 at % Cr, 0.15 at % Zr, 0.04 at % Mg	14	15(a)	7-25(a)	400-500 100-250	- -	- -	- -	0 0	No voids observed in cold-worked plus aged alloy (cross-section analysis).	149, unpubl.
h.p.	38	-	-	~ 200	iL vL	22 2	10^{-6} - 10^{-5} 10^{-5} - 10^{-4}	- -	Vacancy clusters anneal into bubbles or voids.	152
h.p.	0.7 H 1.0 He	- -	- -	20 20	vL vL	2.4 2.4	< 100 < 100	- -	Vacancy clusters form directly in cascade.	155
99.998	0.06 H ⁺ 0.02 H ⁺	- -	- -	70 100 200 250 300	iL	20 35 30-100 75-200 50-300	$8 \times 10^{-5}/t$ $4 \times 10^{-5}/t$ $2 \times 10^{-5}/t$ $2 \times 10^{-6}/t$ $1 \times 10^{-6}/t$	- - - - -	Hexagonal, faulted interstitial loops on (111) planes.	156
h.p. 99.999%	0.03 0.03	- -	- -	20 20	vL vL	5 2.3	- -	- -	Frank sessile vacancy loops equally distributed on (111) planes.	157, 167

TABLE 4. Void and Selected Dislocation Loop Studies in Ion-Irradiated Copper and Copper-Base Alloys
(Continued)

Specimen Purity/ Alloy Concent.	Ion Energy (MeV)	Dose (dpa, K=0.4)	Dose Rate (10^{-4} dpa/s K=0.4)	Irradiation Temp. ($^{\circ}$ C)	Defect*	Mean Diameter (nm)	Density ($10^{20}/m^3$)	Swelling $\Delta V/V$ (%)	Comments	Ref.
h.p.	0.03	-	-	~ 20	vL	2-8	-	-	~ 1 cluster forms per ion	158,
	0.09	-	-	~ 20	vL	2-8	-	-	~ 3 clusters form per ion	160
h.p.	0.005 Ar	-	-	20	1L	1-4	-	-	$\bar{b} = \frac{a}{2} \langle 110 \rangle$; loops may be Ar clusters	159
h.p.	0.15, 0.35	-	-	-130 to 350	-	-	-	-	Damage extended up to 16 times projected range in channelling directions.	161
99.999%	0.03	-	-	20-300 350-400	vL	4.6	$2 \times 10^{-3}/t$	-	Loop number density constant below 300 $^{\circ}$ C. $\langle 111 \rangle$ loops at room temperature; mixture of $\langle 111 \rangle$ and $\langle 110 \rangle$ loops at 400 $^{\circ}$ C.	162, 163
					vL, SFT	5.5	$5 \times 10^{-4}/t$	-		
h.p. 99.99%	0.03	-	-	< -173 -173 to 227 6-295 K	vL	3.6	-	-	~ 0.3 clusters per ion. Possible step-like increase in loop size at irradiation temp. of 200 K. (166)	165, 168
					vL	4.3	-	-		
					vL	3.6	-	-		
99.999%	1.0 H ⁺	-	-	20	1L	-	$1-8 \times 10^4$	-	Defect density vs. depth obtained by cross-section technique. Agreement between observed damage depth distribution and LSS theory only for 1 MeV protons. Only 6% of displaced atoms retained as observable defects.	166
	4.0 Ni	-	-	20	L	1-12	10-400	-		
	60. Ni	-	-	20	L	1-12	-	-		
	1.0 He	-	-	25	vL, 1L	-	-	-		
	5-38 Cu	-	-	25	vL, 1L	-	-	-		
	4. Ni	-	-	25	vL, 1L	-	-	-		
	58. Ni	-	-	25	vL, 1L	-	-	-		

TABLE 4. Void and Selected Dislocation Loop Studies in Ion-Irradiated Copper and Copper-Base Alloys
(Continued)

Specimen Purity/ Alloy Concent.	Ion Energy (MeV)	Dose (dpa, K=0.4)	Dose Rate (10^{-4} dpa/s K=0.4)	Irradiation Temp. ($^{\circ}$ C)	Defect*	Mean Diameter (nm)	Density ($10^{20}/m^3$)	Swelling $\Delta V/V$ (%)	Comments	Ref.
0.6% O	0.03	-	-	20	vL	-	-	-	Damage not greatly affected by impurities.	164
16% Al	0.04	-	-	20	L	1-7.5	-	-	Same type of damages as in pure Cu. Some loops become stacking fault tetrahedra. (164) Other Al concentrations also investigated. (164,169) Defect yield, SFT concentration increases with alloying. (169,170) Different behavior for Cu^{+} vs. W^{+} ions.	103
10% Al	0.03	-	-	20	vL	-	-	-		164
10.4% Al	0.03	-	-	20	vL, SFT	2.5	$1.2 \times 10^{-5}/t$	-		169
15.8% Al	-	-	-	20	vL, SFT	2.2	$1.4 \times 10^{-5}/t$	-		170
10.4% Al	0.09	-	-	20	vL	2.8	-	-		170
15.8% Al	-	-	-	20	vL	2.2	-	-		
2.25% Be	0.03	-	-	20	vL	2.5	-	-	Mostly edge-on Frank loops. Also results for W^{+} ions. Defect yield increased with solute concentration.	169
3.9-7.6% Ge	-	-	-		vL, SFT	2.7-2.4	-	-		
10.1% Ni	-	-	-		vL	2.8	-	-		
8.35% Si	-	-	-		vL, SFT	2.6	-	-		
26.1% Zn	-	-	-		vL, SFT	2.5	-	-		
7.6% Ge	0.09	-	-	20	vL	2.6	-	-		170

* v = void, iL = interstitial loop, vL = vacancy loop/cluster, SFT = stacking fault tetrahedra
(a) dpa calculated assuming a damage efficiency of K=0.3.
t = foil thickness

IV. Fundamental Studies: Radiation Hardening and Resistivity Changes

Recent emphasis on the mechanical properties of irradiated materials combined with ongoing basic studies programs have led to a resurgence in fundamental investigations of the effect of radiation damage on material properties. Experimental tools included in this classification are tensile tests, hardness tests, various ductility tests (Charpy V-notch, disk bend, etc.) and resistivity measurements. The following summarizes some of the work reported in the literature during the past few years.

IV.A. Pure Copper

There have been several recent studies of the effect of neutron irradiation on the yield strength and hardness of copper and copper alloys.^(15,105,107,171-175,186) Mitchell et al.⁽¹⁰⁵⁾ used tensile tests to determine the extent of radiation hardening in copper following a room temperature 14-MeV neutron irradiation. The increase in yield strength appears to vary linearly with the fourth root of neutron fluence, which would indicate that the defect cluster density was proportional to the square root of fluence.⁽¹⁵⁾ Higgy^(172,173) examined radiation hardening in copper and Cu-Al following a 70°C fast neutron irradiation by using tensile tests. A large increase in the critical shear stress due to irradiation to $7 \times 10^{23} \text{ n/m}^2$ was observed. The critical resolved shear stress increased and the work hardening coefficient (n) decreased dramatically during irradiation for strain levels less than 20%.

El-Shanshoury and Mohammed⁽¹⁷¹⁾ and Mohamed et al.⁽¹⁷⁴⁾ measured the Brinell hardness and yield strength of copper irradiated at 40°C with fast neutrons to fluences of $8 \times 10^{23} \text{ n/m}^2$. After an incubation period of $\lesssim 1 \times 10^{21} \text{ n/m}^2$, the hardness of copper was observed to continually increase up to

the maximum fluence. In both studies, the change in the yield strength plotted vs. $(\phi t)^{1/2}$ and $(\phi t)^{1/3}$ was linear up to a fluence of $2 \times 10^{22} \text{ n/m}^2$. At higher fluence levels, the rate of radiation hardening decreased and the yield strength began to approach an asymptotic value ($\Delta\sigma_y \gtrsim 300 \text{ MN/m}^2$).

Brager et al.⁽¹⁰⁷⁾ and Zinkle and Kulcinski^(15,186) have measured the Vickers microhardness (VHN) of copper following a low fluence ($< 8 \times 10^{21} \text{ n/m}^2$) room temperature 14-MeV neutron irradiation. Brager et al. found that the increase in the VHN was linear with the square root of neutron fluence with no incubation period. Zinkle and Kulcinski observed that the change in the VHN was proportional to $(\phi t)^n$, $n = 1/4 \sim 1/2$, with an incubation fluence of $\sim 3 \times 10^{20} \text{ n/m}^2$. The conclusions from the latter investigation are somewhat uncertain due to the low indenter load used to make the measurements (10 g).

Gonzalez and Bisogni⁽¹⁷⁵⁾ found that the increase in yield stress of copper following irradiation with fast neutrons at 77 K up to a maximum fluence of $7 \times 10^{20} \text{ n/m}^2$ was proportional to $(\phi t)^{1/2}$. A tendency for saturation was noted for doses $\gtrsim 5 \times 10^{20} \text{ n/m}^2$. (This may be an indication that the fluence dependence of radiation hardening is changing to $\sim (\phi t)^{1/3}$.)

Blewitt et al.⁽¹⁷⁶⁾ recently monitored the change in yield strength ($\Delta\sigma_y$) of copper irradiated at 4 K with fast neutrons. They observed a large change in yield strength, and this radiation hardening remained essentially constant during an anneal to 600 K. Since dislocation loop formation is strongly temperature dependent, they concluded that radiation hardening must be due to some other type of barrier. Other researchers have indirectly shown that dislocation loops are responsible for radiation hardening in copper,^(15,107) contrary to Blewitt's conclusion. Resistivity and microhardness predictions for

dislocation loop density using existing theoretical models were found to be in good agreement with the observed TEM cluster density following a room temperature 14-MeV neutron irradiation.⁽¹⁵⁾ Ghoniem et al.⁽¹⁰⁶⁾ have recently theoretically investigated the effect of dislocations and dislocation loops on radiation hardening. The model predictions agreed well with experimental observations.⁽¹⁰⁷⁾

Pletnev and Platov⁽¹⁷⁸⁾ have developed a model for dislocation loop size distribution which is in very good agreement with experimental TEM observations. Konstantinov et al.⁽²⁰¹⁾ have recently monitored the microstructure and yield strength of copper irradiated with 23-MeV protons at 220°C. They experimentally found $\Delta\sigma_y \sim (nd_{loop})^{1/2}$ and that the loop density (n) was proportional to $(\phi t)^{0.7}$.

There have been several recent HVEM investigations to determine the displacement energy of copper.^(179,180) It is observed^(179,181,182) that the minimum displacement energy (E_d) is strongly dependent on temperature, decreasing by a factor of 2 as the temperature is increased from 70 K to 500 K. Urban and Yoshida⁽¹⁷⁹⁾ indicated that the dependence on temperature was probably due to low-energy PKA's in the $\langle 110 \rangle$ directions. Therefore, the temperature dependence is expected to be much weaker for high-energy irradiations, in agreement with experiment.⁽¹⁸³⁾

Several resistivity experiments have been performed at low temperatures in order to determine irradiation damage energies of different neutron spectra. This quantity is important for calculations of displacement damage levels (dpa correlations between fission and fusion neutrons). Results have been obtained for d-Be neutrons,⁽¹⁸⁴⁾ 14-MeV neutrons^(185,188) and fast fission neutrons.^(6,185,187) It was found that the high energy neutrons produced

3-3.5 times as much damage in copper as fast fission neutrons, in good agreement with damage energy calculations.⁽⁶⁾ 14-MeV neutrons were about 15% more effective in producing defect damage than d-Be neutrons per unit fluence.

As was mentioned in the introduction of this review, there have been several recent investigations on the effect of incident particle energy on the resultant displacement damage.^(4,6,189-192) The damage efficiency is generally determined by measuring the radiation-induced resistivity increase at liquid helium temperatures. Previously, the "standard" value of the displacement efficiency factor was taken to be $K = 0.8$, regardless of the mass or energy of the irradiating particle.⁽⁵⁾ Measurements on irradiated copper indicate that $K = 0.25$ for high energy neutrons.^(4,6) Resistivity studies of copper irradiated at low temperature with either high energy proton,^(189,190) alpha,⁽¹⁸⁹⁾ or carbon⁽¹⁸⁹⁾ ions or ^{235}U fission fragments⁽¹⁹¹⁾ found that the observed damage energy of the ion bombardments was the same as for fast fission neutrons ($K = 0.25$). Averback et al.⁽¹⁹²⁾ measured damage efficiencies for various ion species incident on copper. They found $K \sim 0.8$ for protons, but then the damage efficiency decreased rapidly with increasing projectile mass. The efficiency became relatively constant for projectiles heavier than Ne with a value of $K \sim 0.3$ for copper.

Investigation of the fluence dependence of defect production during low temperature fast neutron irradiation has shown that the resistivity increase with fluence is less than linear (see Nakagawa⁽¹⁸⁸⁾ and references therein). This effect is caused by the overlap of Frenkel defects at high doses leading to enhanced recombination (radiation annealing), and recent experimental results have been found to be in reasonable agreement with existing theory.⁽¹⁸⁸⁾ Omar et al.⁽¹⁹⁰⁾ found that the resistivity change of pure copper irradiated

with 10-16 MeV protons at 17.5 K varied linearly with dose. It is possible that they were at too low of a dose to be affected by radiation annealing. Birtcher and Blewitt⁽¹⁹¹⁾ observed that the resistivity and length changes of ion irradiated copper were linearly related to each other, even when defect clustering was expected to occur. They concluded that the resistivity change per defect is unaffected by defect clustering. This conclusion is in sharp disagreement with previous clustering studies⁽¹⁹³⁾ (also see discussion on clustering in Ref. 194).

Isochronal annealing studies following low temperature irradiation have found that the amount of recovery occurring in stage I (interstitial migration) increases with dose while the amount of recovery in stage III (vacancy migration) decreases with dose.^(188,195,196) The temperature where stage III recovery occurs also shifts to a lower value.^(188,196)

Maurer⁽¹⁹⁷⁾ has recently given a thorough review of radiation-induced resistivity experiments for copper both with and without magnetic fields. The neutron irradiation temperatures ranged from 4-330 K, with most of the studies concerned with the lower temperatures (relevant for superconducting magnet stabilizers). The maximum fluence was given as $4.5 \times 10^{23} \text{ n/m}^2$. Chaplin and Coltman⁽¹⁹⁸⁾ recently studied resistivity changes in copper due to defects and transmutations during a reactor neutron irradiation near room temperature. For a room temperature irradiation the resistivity change due to defects is known to saturate at high fluence,⁽¹⁹⁹⁾ while the resistivity change due to transmutations increases linearly with fluence. The transmutation contribution was found to exceed the defect contribution at a fluence of $\sim 4 \times 10^{23} \text{ n/m}^2$ ($\sim 0.02 \text{ dpa}$, $K = 0.3$).⁽¹⁹⁸⁾ Therefore, from an engineering point of view it was concluded that transmutation resistivity increases were more important than

defect resistivity increases since a typical copper magnet in a fusion reactor will experience doses much larger than 0.02 dpa during its lifetime.

Lehmann et al.⁽¹⁹⁵⁾ investigated the effect of temperature on damage rate during a high-energy ion irradiation of copper. They found that the initial damage rate at 80 K was 25% of the damage rate found for irradiation near 4 K. The damage production rate was determined to be intermediate between values for electron and fast neutron irradiation.

Theis and Wollenberger⁽²⁰⁰⁾ used resistivity techniques to calculate the number of interstitials which escape correlated (in-cascade) recombination during fast neutron irradiation. This quantity is important for radiation damage modeling. The irradiation was conducted at temperatures between 50 K and 170 K, where the interstitial is mobile but vacancies are not. They estimated that 15% of the total cascade interstitials escaped correlated recombination. Using a similar analysis, Zinkle and Kulcinski⁽¹⁵⁾ estimated that 11-16% of the defects created during a 14-MeV neutron irradiation of copper at room temperature escaped recombination events.

Narayan et al.⁽¹⁶⁶⁾ have examined copper samples in cross-section in an electron microscope following irradiation with various energetic ions. The fraction of displaced ions which were retained in visible defect clusters was computed, and the theoretical depth distribution of damage was compared to TEM observations. The range of 1-MeV protons was in good agreement with LSS theory, whereas LSS theory was found to underestimate the peak damage region for Cu and Ni ions incident on copper by 5-25% depending on the ion energy (greatest disagreement for low energy ions). Knoll⁽⁷⁾ observed similar results during a cross-section investigation of 14-MeV Cu ion irradiation of copper alloys. It was determined by Narayan et al.⁽¹⁶⁶⁾ that electronic stop-

ping of Cu and Ni ions in copper is not proportional to the ion velocity as predicted by LSS theory.

IV.B. Copper Alloys

The effect of alloying on radiation-induced microhardness and yield strength changes in copper following neutron irradiation at or near room temperature has been recently studied by several investigators.^(15,107,171-174,186) Conflicting results have been obtained on the relative importance of solution hardening versus radiation hardening. For example, addition of Al solute to copper has been reported to have either a large^(107,171) or an insignificant^(174,186) effect on the unirradiated strength. Copper alloys containing Al, Ni and Si solutes have generally been found to exhibit radiation hardening similar to that of pure copper.^(107,171,174) Addition of 2 at.% Mg or Sn to copper resulted in a 200-300% increase in the unirradiated yield strength, and also somewhat larger radiation hardening compared to pure copper.⁽¹⁷⁴⁾ This was attributed to the lower stacking fault energy of these alloys. Mohamed et al.⁽¹⁷⁴⁾ also reported that Al, Ge, Mn, Ni and Si solutes had only small effects on both the unirradiated strength and on radiation hardening. Two independent investigations of Cu-5 at.% Mn have resulted in opposite conclusions: Brager et al.⁽¹⁰⁷⁾ found that Mn increased the unirradiated strength of copper and had an insignificant effect on the subsequent radiation hardening. Zinkle and Kulcinski^(15,186) reported that the unirradiated strength of Cu-Mn was similar to that of pure copper, while the irradiated strength was substantially larger due to a shortened incubation fluence for radiation hardening in the alloy.

The fluence dependence of radiation hardening in copper alloys is similar to that reported for pure copper -- various reports have found that radiation

hardening in the temperature range 20-70°C is proportional to $(\phi t)^{1/2}$, $(\phi t)^{1/3}$ or $(\phi t)^{1/4}$. Some of the variance in dose dependence may be due to the fluence range investigated. Several results indicate that the radiation hardening rate changes with fluence, and saturation may start occurring for fluences $\sim 3 \times 10^{22}$ n/m².^(171,174) It is uncertain whether there is an incubation fluence prior to the occurrence of observable radiation hardening in copper alloys, since most investigations have not examined very low fluence behavior. Zinkle and Kulcinski^(15,186) found that the addition of 5 at.% Al, Mn or Ni solute to copper decreased the incubation fluence for observable radiation hardening from 3×10^{20} n/m² to less than 1×10^{20} n/m². This was attributed to short range ordering effects.⁽¹⁸⁶⁾ In general, the slope of the radiation hardening versus fluence curves appear to be roughly the same for pure copper and all single phase copper alloys. This may be an indication of equivalent damage production rates in all of these materials.

Resistivity measurements have been conducted on dilute copper alloys in order to identify nonpurity atom trapping/detrapping mechanisms and to measure solute atom-point defect capture radii.^(182,202-206) These quantities are important for the determination of solute atom enhancement of point defect recombination. The capture radii of impurities were found to decrease with increasing irradiation temperature in the range 50-170 K. This was attributed to radiation-induced detrapping.⁽²⁰²⁾ The capture radii of most impurities became zero at about 110 K. Solute trapping energies as large as 0.24 eV have been observed.⁽¹⁴⁸⁾ Thorough reviews of this subject may be found elsewhere.^(182,204)

V. Concluding Remarks

As is evidenced by the preceding sections, a rather large volume of experimental data has been published on radiation effects on copper and its alloys. Table 5 lists the number of radiation damage studies presented in this review according to irradiating species and observed radiation effect. Dislocation loop formation following irradiation was not fully reviewed in this report due to the presence of several extensive reviews available in the literature (in particular, following neutron irradiation). (82-84,151)

Examination of the radiation damage literature reveals that there is presently no known high-fluence neutron data for copper or copper alloys (see Table 6 below). It is known that pure copper swells readily at very low neutron doses (< 0.1 dpa). However, the steady-state swelling rate can not be determined without higher fluence data. Charged particle studies indicate that the incubation dose for void swelling is from 0 to ~ 5 dpa, and the linear swelling rate is similar to that observed in stainless steel (Table 6). For copper alloys, it generally appears that low amounts of solute ($\lesssim 0.1\%$) enhance void swelling while large amounts ($\gtrsim 1\%$) suppress swelling.

The authors of this report are aware of several extensive fast neutron irradiation programs which are currently being conducted on copper and copper alloys. Details of the materials being irradiated and the irradiation conditions are available in Refs. 207-210. High-fluence irradiation data from these investigations at temperatures of 400-515°C should become available by the end of 1985.

Acknowledgment

This work was performed under appointment to the Magnetic Fusion Energy Technology Fellowship Program and with funds supplied by the U.S. Department of Energy.

Table 5. Number of Experimental Studies of Radiation Effects in Copper and Copper Alloys

	<u>Solute Segregation</u>	<u>Void</u>	<u>Loop*</u>
Electron	24	12	15
Ion	11	10	21
Neutron	<u>28</u>	<u>12</u>	<u>17</u>
	63 (16 alloys)	34	53

*partial listing

Table 6. Summary of General Loop and Void Observations in Irradiated Copper

<u>Irradiating Species</u>	<u>Loop Character</u>	<u>Max. Dose for Void Swelling</u>	<u>Swelling Rate</u>	<u>Max. Observed Swelling</u>
Electron	Interstitial	95 dpa (K = 0.8)	0.5-0.8%/dpa (K = 0.8)	14% 17% (Ar preinject)
Ion	Vacancy	> 30 dpa (K = 0.3)	0.2-0.6%/dpa (K = 0.3)	9% 14% (He preinject)
Neutron	i,v mix	0.2 dpa (K = 0.3)	?	0.5%

References

1. F.W. Wiffen and R.E. Gold (Eds.), Copper and Copper Alloys for Fusion Reactor Applications (DOE-OFE Workshop Proceedings) Oak Ridge National Laboratory CONF-830466 (June 1984).
2. J.W. Corbett, Electron Radiation Damage in Semiconductors and Metals, Solid State Physics Supplement 7, Academic Press (1966).
3. R.W. Knoll, "A Literature Review of Radiation Damage Data in Copper," University of Wisconsin Fusion Engineering Report UWFD-384 (Oct. 1980).
4. J.H. Kinney, M.W. Guinan and Z.A. Munir, "Defect Production Efficiencies in Thermal Neutron Irradiated Copper and Molybdenum," Third Topical Meeting on Fusion Reactor Materials, Albuquerque, NM (Sept. 1983), J. Nucl. Mater. 122/123 (1984) 1028-1032.
5. I.M. Torrens and M.T. Robinson in Radiation-Induced Voids in Metals, J.W. Corbett and L.C. Iannello (Eds.) US AEC Technical Information Center CONF-710601 (1972) 739-756.
6. M.W. Guinan and J.H. Kinney, J. Nucl. Mater. 108/109 (1982) 95-103.
7. R.W. Knoll, "Effects of Heavy Ion Irradiation on the Phase Stability of Several Copper-Base Alloys," Ph.D. Thesis, Nuclear Engineering Department, University of Wisconsin-Madison (1981); available as UWFD-436. Most of the irradiated Cu-Be results are contained in "Precipitation in Cu-3.4 at.% Be Solid Solution During Heavy Ion Irradiation, Parts I and II," which has been submitted to the J. Nucl. Mater., June 1984.
8. K.C. Russell, "Phase Stability Under Irradiation, Part II - Experimental," to be published in Progress in Materials Science, J. Christian, P. Haasen and T.B. Massalski (Eds.), Pergamon Press, Oxford (1983).
9. H.W. King, J. Mater. Sci. 1 (1966) 79-90.
10. T. Takeyama, S. Ohnuki and H. Takahashi, Scripta Met. 14 (1980) 1105-1110.
11. H. Takahashi, S. Ohnuki and T. Takeyama, J. Nucl. Mater. 103/104 (1981) 1415-1420.
12. M.S. Wechsler and R.H. Kernohan, J. Phys. Chem. Sol. 7 (1958) 307-326.
13. R.H. Kernohan and M.S. Wechsler, J. Phys. Chem. Sol. 18 (1961) 175-180; also Radiation Damage in Solids, Vol. II, IAEA, Vienna (1962) 81-103.
14. C. Kinoshita, K. Shinohara and S. Kitajima, Ann. Rep. Res. React. Inst. Kyoto Univ. (Japan) 9 No. 8 (1976) 150-154.

15. S.J. Zinkle and G.L. Kulcinski, "14-MeV Neutron Irradiation of Copper Alloys," J. Nucl. Mater. 122/123 (1984) 449-454.
16. M.K. Sardar et al., Scripta Met. 16 (1982) 1035.
17. A.J. Friedman et al., Phys. Rev. B 6 No. 2 (1972) 356-363.
18. G. Oleownik and W. Schüle in Fund. Aspects of Radiation Damage in Metals, Vol. 1, M.T. Robinson and F.W. Young (Eds.), Gatlinburg, TN (1975) CONF-751006-P1, p. 341.
19. R.H. Zee and P. Wilkes, Phil. Mag. A42 (1980) 463.
20. R.H. Zee and P. Wilkes, J. Nucl. Mater. 97 (1981) 179.
21. R.H. Zee, "Radiation Induced Order-Disorder Phase Transformation," Ph.D. Thesis, Nuclear Engineering Dept., University of Wisconsin-Madison (May 1981) UWFD-418.
22. M.W. Guinan, J.H. Kinney, R.A. Van Konynenburg and A.C. Damask, J. Nucl. Mater. 103/104 (1981) 1217-1220.
23. C.A. English and M.L. Jenkins, J. Nucl. Mater. 96 (1981) 341-357.
24. M.A. Kirk and T.H. Blewitt, Met. Trans. 9A (1978) 1729.
25. M.Z. Hammed, R.E. Smallman and M.H. Loretto, Phil. Mag. A46 (1982) 707, 717.
26. H.J. Fenzl, J.M. Welter and K. Boning, 1st European Conf. on Condensed Matter European Phys. Soc., Italian Nat. Res. Council (14-17 Sept. 1971) Florence, Italy and Geneva, Switzerland.
27. G.T. Murray and W.E. Taylor, Acta Met. 2 (1954) 52-62.
28. L.N. Bystrov, L.I. Ivanov and Yu. M. Platov, Physics of Metals and Metallogr. 25 No. 5 (1968) 194-197 (transl. of Fiz. Metal. Metalloved. 25 (1968) 950-953).
29. H. Yoshida, Phil. Mag. 19 (1969) 987-991.
30. H. Yoshida, H. Kodaka and K. Miyata, Ann. Report Res. Reactor Inst. Kyoto Univ. (Japan) 4 (1971) 119-122.
31. H. Yoshida, S. Yamamoto, Y. Murakami and H. Kodaka, Trans. Jap. Inst. Metals 12 No. 4 (1971) 229-237.
32. H. Yoshida and T. Sagane, J. Nucl. Sci. Tech. 9 (1972) 1-6.

33. H. Yoshida in Solid to Solid Phase Transformations, Proc. of an International Conference, Pittsburgh, PA (August 1981), H.I. Aaronson et al. (Eds.) TMS-AIME (1982) 299-303; also Ann. Reports Res. Reactor Institute, Kyoto Univ. (Japan) 12 (1979) 83-113.
34. W.V. Lensa, A. Bartels, F. Dworschak and H. Wollenberger, J. Nucl. Mater. 71 (1979) 78-81.
35. A. Bartels, F. Dworschak, H.P. Abromeit and H. Wollenberger, J. Nucl. Mater. 83 (1979) 24-34.
36. R.W. Knoll, P. Wilkes and G.L. Kulcinski, in Phase Stability During Irradiation, AIME (1981) 123-137.
37. R.A. Johnson and N.Q. Lam, Phys. Rev. B 13, No. 10 (1976) 4364.
38. R. Koch, R.P. Wahi and H. Wollenberger, J. Nucl. Mater. 103/104 (1981) 1211-1216.
39. R.P. Wahi and H. Wollenberger, J. Nucl. Mater. 113 (1983) 207-210.
40. H-J. Gudladt, V. Naundorf, M-P. Macht and H. Wollenberger, J. Nucl. Mater. 118 (1983) 73-77.
41. M-P. Macht, V. Naundorf and H. Wollenberger, J. Nucl. Mater. 103/104 (1981) 1487.
42. M-P. Macht, V. Naundorf, R.P. Wahi and H. Wollenberger, J. Nucl. Mater. 122/123 (1984) 698-702.
43. C. Kinoshita, L.W. Hobbs and T.E. Mitchell, in Phase Stability During Irradiation, AIME (1981) 561-575.
44. G.R. Piercy, J. Phys. Chem. Solids 23 (1962) 463-477.
45. A. Blaise, J. de Physique 26 (1965) 361-365.
46. L.M. Brown, G.R. Woolhouse and U. Valdre, Phil. Mag. 17 (1968) 781-789.
47. G.R. Woolhouse, Nature 220 (1968) 573-574.
48. G.R. Woolhouse and M. Ipohorski, Proc. Roy. Soc. London A324 (1971) 415-431.
49. R.E. Rovinskii, V.E. Rogalin, V.M. Rosenberg and M.D. Teplitskii, Fiz Khim Obrab. Mater., June 1980 (3) 7-11.
50. J.M. Denney, Phys. Rev. 92 No. 2 (1953) 531.
51. J.M. Denney Phys. Rev. 94 No. 5 (1954) 1417-1418.

52. A. Boltax, in Radiation Effects on Materials, Vol. 1, ASTM STP 208 (1956) 183-190.
53. A. Boltax, Nucl. Appl. 1 (1965) 337-347.
54. T.H. Gould and D.H. Vincent, J. de Physique 35, Supplement C6, No. 12 (1974) 315-319.
55. T. Takeyama, S. Ohnuki and H. Takahashi, J. Nucl. Mater. 89 (1980) 253-262.
56. H. Saka, Phil. Mag. A48 (1983) 239-250.
57. L. Rivaud, A.H. Eltoukhy and J.E. Greene, et al., Rad. Effects 61 (1982) 83-92.
58. W. Schüle, P. Spindler and E. Lang, Z. Metallkunde 66 (1975) 50-56.
59. R. Poerschke and H. Wollenberger, Thin Solid Films, 25 (1975) 167-170.
60. R. Poerschke and H. Wollenberger, Rad. Effects 24 (1975) 217-221.
61. R. Poersche and H. Wollenberger, Fund. Aspects of Radiation Damage in Metals, Vol. II, M.T. Robinson and F.W. Young, Jr. (Eds.), Gatlinburg, TN (1975), CONF-751006-P2, pp. 1070-1076.
62. R. Poerschke and H. Wollenberger, J. Phys. F 6 (1976) 27-41.
63. R. Poerschke and H. Wollenberger, Rad. Effects 49 (1980) 225-232.
64. Y. Adda, M. Beyeler and G. Brebec, Thin Solid Films 25 (1975) 107-156.
65. W. Wagner, R. Poerschke and H. Wollenberger, J. Phys. F 12 (1982) 405-424.
66. D.G. Swartzfager, S.B. Ziemecki and M.J. Kelley, J. Vac. Sci. Technology 19 No. 2 (Jul./Aug. 1981) 185-191.
67. H. Shimizu et al., J. Japan Inst. of Metals (Nippon Kinzoku Gakkai) 45 (Jan.-Jun. 1981) 210.
68. H. Shimizu, N. Koyama and Y. Ishida, J. Japan Inst. of Metals (Nippon Kinzoku Gakkai) 45 (Jul.-Dec. 1981) 768.
69. L.E. Rehn, W. Wagner and H. Wiedersich, Script Met. 15 (1981) 683-687.
70. N.Q. Lam and H. Wiedersich, Rad. Effects Letters, 67 No. 4 (1982) 107-112.
71. T. Takeyama, Bull. Japan Inst. Met. (Nippon Kinzoku Gakkai Kaiho) 22 No. 2 (1983) 135-137.

72. K. Chountas et al., Rad. Effects Letters 43 (1979) 249-251.
73. A.M. Shalaev, Metallofizika, No. 71 (1978) 3-11.
74. R.H. Zee, M.W. Guinan and G.L. Kulcinski, J. Nucl. Mater. 114 (1983) 190-198.
75. T. Takeyama, in New Trends in Electron Microscopy in Atom Resolution, Materials Science and Biology, (Conf. Proc.), H. Hashimoto et al. (Eds.), Dalian, China (July 1981), Science Press, Beijing, China (1982) 78-86.
76. J. Hillairet, E. Balanzat, J. Bigot and H.U. Künzi, J. de Physique Supplement 41, No. C8 (1980) 854-857.
77. W. Schüle, E. Lang, D. Donner and H. Penkuhn, Rad. Effects 2 (1970) 151-163.
78. K. Salamon and W. Schüle, Rad. Effects 16 (1972) 45-55.
79. S. Takamuro and S. Okuda, Rad. Effects 17 (1973) 151-158.
80. R. Poerschke and H. Wollenberger, J. Nucl. Mater. 74 (1978) 48-61.
81. A.C. Damask, J. Gilbert and H. Herman, Rad. Effects 26 (1975) 89.
82. M. Rühle, Proc. of the Symp. on Radiation Damage in Reactor Materials, Vol. 1 (Vienna, 1969) 113-158.
83. M. Wilkens, "Studies of Point Defect Clusters by TEM," in Vacancies and Interstitials in Metals, Seeger et al. (Eds.), North-Holland (1970) p. 485.
84. B.L. Eyre, J. Phys. F 3 (1973) 422.
85. J.L. Brimhall and B. Mastell, J. Nucl. Mater. 29 (1969) 123-125.
86. V. Levy, J. Mathie, A. Risbet, R. Levy and J.P. Poirier, in Voids Formed by Irradiation of Reactor Materials, S.F. Pugh (Ed.), British Nuclear Energy Society (1971) 64-68.
87. Y. Adda, Radiation-Induced Voids in Metals, J.W. Corbett and L.C. Ianniello (Eds.), AEC Symposium Series No. 26 (1972) 31-81.
88. A. Wolfenden, Rad. Effects 15 (1972) 255-258.
89. J.L. Brimhall and H.E. Kissinger, Rad. Effects 15 (1972) 259-272.
90. M. Labbe and J.P. Poirier, J. Nucl. Mater. 46 (1973) 86-98.

91. M. Labbe, G. Brebec and J.P. Poirier, J. Nucl. Mater. 49 (1973/74) 232-234.
92. R.B. Adamson, W.L. Bell and P.C. Kelly, J. Nucl. Mater 92 (1980) 149-154.
93. J.W. Muncie, "Low Dose Fast Neutron Irradiation of Copper at Elevated Temperatures," 1978 Modern Metallography Conf. and Exhibition, Birmingham, England (Sept. 1978). Most of this thesis work was later described by English (Ref. 94).
94. C.A. English, J. Nucl. Mater. 108/109 (1982) 104-123.
95. M. Eldrup, J.H. Evans, O.E. Mogensen and B.N. Singh, Rad. Effects 54 (1981) 65-80.
96. N. Yoshida, K. Kitajima and E. Kuramoto, "Evolution of Damage Structures under 14-MeV Neutron, 4-MeV Ni Ion and 1.25-MeV Electron Irradiation," J. Nucl. Mater. 122/123 (1984) 664-668.
97. L.D. Hulet, Jr., T.O. Baldwin, J.C. Crump, III and F.W. Young, Jr., J. Applied Physics 39 No. 8 (1968) 3945-3954.
98. M. Ruhle, F. Haussermann and M. Rapp, Phys. Stat. Sol. 39 (1970) 609-620.
99. B.C. Larson and F.W. Young, Jr., in Radiation Induced Voids in Metals, J.W. Corbett and L.C. Ianniello (Eds.), AEC Symposium Series No. 26, (1972) 672-683.
100. J.B. Mitchell, C.M. Logan and C.J. Echer, J. Nucl. Mater 48 (1973) 139-142.
101. W.B. Gauster, S. Mantl, T. Schober and W. Triftshauser, Fundamental Aspects of Radiation Damage in Metals, Vol. 1, M.T. Robinson and F.W. Young (Eds.) Gatlinburg, TN (1975) CONF-751006-P1, 1143-1149.
102. D.E. Barry and B.L. Eyre, Phil. Mag. 22 (1970) 717-737.
103. L.M. Howe and M. Rainville, Rad. Effects 16 (1972) 203-209.
104. J. Narayan and S.M. Ohr, J. Nucl. Mater. 85/86 (1979) 515-519.
105. J.B. Mitchell et al., Radiation Effects and Tritium Technology for Fusion Reactors, J.S. Watson and F.W. Wiffen (Eds.), Gatlinburg, TN, Vol. II (Oct. 1975) 172.
106. N.M. Ghoniem et al., ASTM STP 782 Scottsdale, AZ (1982) p. 1054.
107. H.R. Brager, F.A. Garner and N.F. Panayotou, J. Nucl. Mater. 103/104 (1981) 995.

108. B. von Guerard and J. Peisl, in Fundamental Aspects of Radiation Damage in Metals, M.T. Robinson and F.W. Young (Eds.), CONF-751006-P1, Vol. I (1975) 309.
109. J.B. Roberto, J. Narayan and M.J. Saltmarsh, Radiation Effects and Tritium Technology for Fusion Reactors, J.S. Watson and F.W. Wiffen (Eds.) Gatlinburg, TN, Vol. II (Oct. 1975) 159.
110. B.C. Larson and F.W. Young, Jr., J. Appl. Phys. 48 (1977) 880-886.
111. M. Ruhle and J.C. Crump, III, Phys. Stat. Sol. A2 (1970) 257.
112. R.H. Howell, Phys. Rev. B 22 (1980) 1722.
113. M. Ipohorski and L.M. Brown, Phil. Mag. 22 (1970) 931.
114. M.J. Makin in Voids Formed by Irradiation of Reactor Materials, S.F. Pugh (Ed.), British Nuclear Engineering Society (1971) 269-274.
115. T. Leffers, B.N. Singh, S.N. Buckley and S.A. Manthorpe, J. Nucl. Mater. 118 (1983) 60-67.
116. S.B. Fisher, Rad. Effects 7 (1971) 173-177.
117. E. Kenik and T.E. Mitchell, Rad. Effects 24 (1975) 155-160.
118. L.D. Glowinski, J. Nucl. Mater. 61 (1976) 8-21.
119. P. Barlow, "Radiation Damage in Pure FCC Metals and Alloys in HVEM," Ph.D. Thesis, University of Sussex, England (1977).
120. T. Leffers, B.N. Singh and P. Barlow, Riso-M-1937, Research Establishment Riso, Roskilde, Denmark (May 1977).
121. K. Hinode, S. Tanigawa and M. Doyama, Rad. Effects 32 (1977) 73-77.
122. S.B. Fisher, R.J. White and K.M. Miller, Phil. Mag. A40 (1979) 239-255.
123. T. Leffers, B.N. Singh, S.N. Buckley, S.A. Manthorpe, Irradiation Behavior of Metallic Materials for Fast Breeder Core Components (Intern. Conf.), Corse, France (1979) 235-240.
124. S.N. Buckley, M.J. Makin and S.A. Manthorpe, Rad. Effects 59 (1982) 203-209.
125. B.N. Singh and T. Leffers, Proc. of Sixth International Conference on HVEM, Antwerp, 1980, Electron Microscopy 4 (1980) 262-265.
126. P. Barlow, T. Leffers and B.N. Singh, Riso-M-2129, Research Establishment Riso, Roskilde, Denmark (August 1978).

127. M.J. Makin, *Phil. Mag.* 18 (1968) 637-653.
128. M. Ipohorski and M.S. Spring, *Phil. Mag.* 20 (1969) 937-941.
129. Y. Shimomura, K. Tanaka, M. Okada and T. Kino, *Jap. J. Appl. Physics*, 18 No. 10 (Oct. 1979) 1891-1895.
130. A.Y. Stathopoulos, S.M. Murphy, M.H. Wood, R. Bullough and C.A. English, *J. Nucl. Mater.* 110 (1982) 301-308.
131. N. Yoshida and M. Kiritani, *J. Phys. Soc. Japan* 38 (1975) 1220.
132. H. Fujita, T. Sakata and H. Fukuyo, *Jap. J. Appl. Phys.* 21 No. 4 (1982) L235-L236.
133. M. Kiritani, K. Urban and N. Yoshida, *Rad. Effects* 61 (1982) 117-126.
134. W. Jager, W. Frank and K. Urban, *Rad. Effects* 46 (1980) 47-58.
135. S.M. Ohr, *J. Nucl. Mater.* 69/70 (1978) 830.
136. P. Ehrhardt and U. Schlagheck, *J. Phys. F* 4 (1974) 1589.
137. H-G. Haubold and D. Martinsen, *J. Nucl. Mater.* 69/70 (1978) 644-649; also see *J. Appl. Crystallogr.* 11 (1978) 592-596.
138. T. Kosel and J. Washburn in *Fund. Aspects of Radiation Damage in Metals*, Vol. II, M.T. Robinson and F.W. Young (Eds.) Gatlinburg, TN, (Oct. 1975) CONF-751006-P2, 903-909.
139. C. Kinoshita and T.E. Mitchell, *Electron Microscopy 1980*, Vol. 4, p. 236.
140. T. Mukai and T.E. Mitchell, *Phil. Mag.* A45 (1982) 741-751.
141. D.J. Mazey and F. Menzinger, *J. Nucl. Mater.* 48 (1973) 15-20.
142. K-H. Leister, "Influence of Solutes on Heavy Ion Induced Void-Swelling in Binary Copper Alloys," Ph.D. Thesis, Kernforschungszentrum Karlsruhe (May 1983), KfK Report 3499; also K-H. Leister, K. Exel, W. Humbach, K. Schmelz and K. Ehrlich, "Void Swelling in Binary Copper Alloys," 1981 Scientific Report from Gesellschaft für Schwerionenforschung (March 1982) ISSN 0174-0814, p. 3.2.
143. J.M. Lanore, L. Glowinski, A. Risbet, P. Regnier, J. Flament, V. Levy and Y. Adda, *Fund. Aspects of Radiation Damage in Metals*, Vol. 2, M.T. Robinson and F.W. Young (Eds.), Gatlinburg, TN (1975) CONF-751006-P2, 1169-1179.
144. L.D. Glowinski, C. Fiche and M. Lott, *J. Nucl. Mater.* 47 (1973) 295-310.

145. L.D. Glowinski and C. Fiche, J. Nucl. Mater. 61 (1976) 22-28.
146. L.D. Glowinski and C. Fishe, J. Nucl. Mater. 61 (1976) 29-40.
147. M.F. Felson and P. Regnier, Scripta Met. 11 (1977) 133-136.
148. B. Badger, Jr., D.L. Plumton, S.J. Zinkle, R.L. Sindelar, G.L. Kulcinski, R.A. Dodd and W.G. Wolfer, "Experimental Investigation of the Effect of Injected Interstitials on Void Nucleation," 12th Intern. Symp. on the Effects of Radiation on Materials, J.S. Perrin, F.A. Garner and J.J. Koziol (Eds.), Williamsburg, VA (June 1984), to be published as a Special Technical Publication by ASTM.
149. S.J. Zinkle, R.A. Dodd and G.L. Kulcinski, "Comparison of Thermal and Irradiated Behavior of High-Strength, High-Conductivity Copper Alloys," 12th Intern. Symp. on the Effects of Radiation on Materials, J.S. Perrin, F.A. Garner and J.J. Koziol (Eds.), Williamsburg, VA (June 1984), to be published as a Special Technical Publication by ASTM.
150. H. Venker, P. Giesecke and K. Ehrlich, Radiation Effects in Breeder Reactor Structural Materials (Int. Conf.), Bleiberg and Bennett (Eds.), Scottsdale, AZ (June 1977), TMS-AIME, 415-420.
151. A.Y. Stathopoulos, "The Study of Heavy Ion Damage in Pure Copper," AERE Report R9784 (June 1980), Harwell, England.
152. R.S. Barnes and D.J. Mazey, Phil. Mag. 5 (1960) 1247.
153. H. Diepers, Phys. Stat. Sol. 24 (1967) 623.
154. J. Diehl, H. Diepers and B. Hertel, Can. J. Physics 46 (1968) 647.
155. K.L. Merkle, Phys. Stat. Sol. 18 (1966) 173.
156. D.J. Mazey and R.S. Barnes, Phil. Mag. 17 (1968) 387.
157. M.M. Wilson, Rad. Effects 1 (1969) 207-208.
158. M.M. Wilson, Phil. Mag. 24 (1971) 1023-1037.
159. J.M. Rojo and L. Bru, Phil. Mag. 25 (1972) 1409.
160. M.M. Wilson and P.B. Hirsch, Phil. Mag. 25 (1972) 983-991.
161. D.K. Sood and G. Dearnaley, J. Vac. Sci. and Tech. 12, No. 1 (1975) 463.
162. C.A. English, B.L. Eyre and J. Summers, Phil. Mag. 34 (1976) 603-614.
163. C.A. English, B.L. Eyre, J. Summers and H. Wadley in Fundamental Aspects of Radiation Damage in Metals, Vol. 2, M.T. Robinson and F.W. Young (Eds.) Gatlinburg, TN (1975) CONF-751006-P2, 910-917.

164. C.A. English, B.L. Eyre, H. Wadley and A.Y. Stathopoulos in Fundamental Aspects of Radiation Damage in Metals, Vol. 2, M.T. Robinson and F.W. Young (Eds.) Gatlinburg, TN (1975) CONF-751006-P2, 918-924.
165. R. Schindler, M. Rühle, W. Frank and M. Wilkens, Commun. on Phys. 1 (1976) 119-123.
166. J. Narayan, O.S. Oen and T.S. Noggle, J. Nucl. Mater. 71 (1977) 160-170.
167. A.Y. Stathopoulos, C.A. English, B.L. Eyre and P.B. Hirsch, Phil. Mag. A44 (1981) 285-308.
168. A. Laupheimer, W. Frank, M. Rühle, A. Seeger and M. Wilkens, Rad. Effects Letters 67, No. 3 (1981) 95-99.
169. A.Y. Stathopoulos, C.A. English, B.L. Eyre and P.B. Hirsch, Phil. Mag. A44 (1981) 309-322.
170. A.Y. Stathopoulos and C.A. English, J. Nucl. Mater. 108/109 (1982) 69-70.
171. I.A. El-Shanshoury and H. Mohammed, Soviet Atomic Energy 25 No. 1 (1968) 765-770; also I.A. El-Shanshoury, J. Nucl. Mater. 45 (1972) 245-257.
172. H.R. Higgy, J. Nucl. Mater. 107 (1982) 90-96.
173. H.R. Higgy, J. Nucl. Mater. 115 (1983) 307-312.
174. M.G. Mohamed, A.M. Hammad and F.H. Hammad, Trans. Indian Inst. Metals, 36, No. 3 (June 1982) 258-262.
175. H.C. Gonzalez and E.A. Bisogni, Phys. Stat. Sol.(a) 62 (1980) 351-361.
176. T.J. Blewitt, T.L. Scott and R.A. Conner, Jr., J. Nucl. Mater 108/109 (1982) 442.
177. R.I. Lekht, Mashinovedenie, No. 3, (May-June 1983) 117-122.
178. M.N. Pletnev and Yu.M. Platov, Phys. Met. Metallogr. 40, No. 2 (1975) 64-69 (translation of Fiz. metal. metalloved.).
179. K. Urban and N. Yoshida, Phil. Mag. 44A (1981) 1193-1212.
180. W.E. King, K.L. Merkle and M. Meshii, J. Nucl. Mater. 117 (1983) 12-25.
181. P. Jung, Rad. Effects 59 (1981) 103-104.
182. H. Wollenberger in Irradiation Behavior of Metallic Materials for Fast Breeder Core Components (Intern. Conf.) Corse, France (June 1979) p. 95.

183. G. Roth, H. Wollenberger, Ch. Zeckau and K. Lucke, Rad. Effects 26 (1975) 141.
184. J.B. Roberto, C.E. Klabunde, J.M. Williams, R.R. Coltman, Jr., M.J. Saltmarsh and C.B. Fulmer, Appl. Phys. Lett. 30 (1977) 509-511.
185. R.A. Van Konynenberg, M.W. Guinan and J.H. Kinney, J. Nucl. Mater. 103/104 (1981) 739-744.
186. S.J. Zinkle and G.L. Kulcinski, "14-MeV Neutron Radiation-Induced Microhardness Changes in Copper Alloys," Symposium on the Use of Nonstandard Subsize Specimens for Irradiated Testing, Albuquerque, NM (Sept. 1983); to be published by ASTM.
187. R.R. Coltman, Jr., C.E. Klabunde and J.M. Williams, J. Nucl. Mater. 99 (1981) 284-293.
188. M. Nakagawa, J. Nucl. Mater. 108/109 (1982) 194-200.
189. H. Sakairi et al., J. Phys. Soc. Japan 43 (1977) 999-1005.
190. A.M. Omar, J.E. Robinson and D.A. Thompson, J. Nucl. Mater. 84 (1979) 173-182.
191. R.C. Birtcher and T.H. Blewitt, J. Nucl. Mater. 98 (1981) 63-70.
192. R.S. Averback, R. Benedek and K.L. Merkle, Phys. Rev. B 18 (1978) 4156-4171; and J. Nucl. Mater. 69/70 (1978) 786-789.
193. L. Thompson et al., Rad. Effects 20 (1973) 111.
194. S.J. Zinkle, "Electrical Resistivity of Dislocations in Metals," UWFD-538 (1983).
195. M. Lehmann et al., Rad. Effects 46 (1980) 227.
196. C.S.B. Piani and J.C. Aspelng, Rad. Effects 69 (1983) 19-28, 29-38.
197. W. Maurer, "Neutron Irradiation Effects on Superconducting and Stabilizing Materials for Fusion Magnets," Institut für Technische Physik, Kernforschungszentrum Karlsruhe (May 1984) KfK 3733.
198. R.L. Chaplin and R.R. Coltman, Jr., J. Nucl. Mater. 108/109 (1982) 175-182.
199. B. McGrath et al., Nucl. Instr. Methods 136 (1976) 575.
200. U. Theis and H. Wollenberger, J. Nucl. Mater. 88 (1980) 121.
201. I.O. Konstantinov, V.S. Kharbarov and V.I. Shcherbak, Fiz. Khim. Obrab. Mater. No. 3 (1982) 135-138.

202. F. Dworschak, R. Lennartz and H. Wollenberger, J. Phys. F 5 (1975) 400.
203. F. Maury et al., Rad. Effects 51 (1980) 57-68.
204. H. Wollenberger, J. Nucl. Mater 69/70 (1978) 362-371.
205. A. Bartels et al., J. Phys. F. 12 (1982) 641-648.
206. G. Wehr, G. Sieber and K. Boning, J. Phys. F 6 No. 11 (1976) 2133-2150.
207. H.R. Brager and F.A. Garner (HEDL), "Irradiation of Copper Alloys in FFTF," DAFS Quarterly Progress Report DOE/ER-0046/17, (May 1984) p. 133 (FFTF, 6-60 dpa (K = 0.3), 450°C).
208. F.W. Clinard, Jr. (LANL), "Copper Alloy Irradiation Studies in Support of CRFPR First Wall," in Ref. 1, p. 347 (EBR-II, ~ 1-6 dpa (K = 0.3), 385°C).
209. O.K. Harling and N.J. Grant (MIT), "The MIT Neutron Irradiation Effects Program with Copper Alloys," in Ref. 1, p. 353 (EBR-II, 6-11 dpa (K = 0.3), 400°C).
210. J.B. Whitley (SNLA), "The High Heat Flux Components Program," in Ref. 1, p. 379 (FFTF and EBR-II, 0.4-1 dpa (K = 0.3), 400, 515°C).